

Cite this: *Nanoscale Adv.*, 2024, 6, 51

Green synthesis trends and potential applications of bimetallic nanoparticles towards the sustainable development goals 2030

Mariana Larrañaga-Tapia,^{†a} Benjamín Betancourt-Tovar,^{†a} Marcelo Videia,^{ⓑ a} Marilena Antunes-Ricardo^{ab} and Jorge L. Cholula-Díaz^{ⓑ *a}

The world faces threats that the United Nations has classified into 17 categories with different objectives as solutions for each challenge that are enclosed in the Sustainable Development Goals (SDGs). These actions involved the widespread use of science and technology as pathways to ensure their implementation. In this regard, sustainability science seeks the research community's contribution to addressing sustainable development challenges. Specifically, nanotechnology has been recognized as a key tool to provide disruptive and effective strategies to reach the SDGs. This review proposes the application of bimetallic nanoparticle substances capable of providing possible solutions to achieve target SDG 3: good health and well-being, SDG 6: clean water and sanitation, and SDG 12: responsible consumption and production. Furthermore, the term green nanotechnology is introduced in each section to exemplify how green synthesized bimetallic nanoparticles have been used to resolve each target SDG. This review also outlines the current scenario regarding the utilization of metallic nanomaterials in the market, together with the upscaling challenges and the lack of understanding of the long-term effects and hazards to the environment regarding bimetallic nanoparticles.

Received 9th September 2023
Accepted 8th November 2023

DOI: 10.1039/d3na00761h

rsc.li/nanoscale-advances

1 Introduction

In September 2015, 193 states adopted the United Nations (UN) 2030 Agenda for Sustainable Development.¹ This agenda is a comprehensive policy blueprint that aims for all nations to be economically prosperous, socially inclusive, environmentally sustainable, and well-governed by 2030. To achieve these objectives, 17 Sustainable Development Goals (SDGs) were established and divided into four main pillars: social, economic, environmental, and governance.² The social pillar comprises the first seven goals of the agenda, focusing on tackling poverty, bad nutrition, a deficit in ensuring healthy lives, deficiency in education systems, gender inequality, and lack of clean water and sanitation and aims to provide access to sustainable energy. The economic pillar encompasses goals 8 to 12, which involve decent work, economic growth, innovation, infrastructure, income inequalities, sustainable cities, and responsible consumption and production. Goals 13 to 15 comprise the environmental pillar and target how to take care of our planet in terms of climate, life underwater, and land, respectively. Finally, the governance pillar comprises goals 16

and 17 related to promoting peace and strong institutions and partnerships, respectively, aligned with the previous SDGs.

To accomplish the SDGs, the UN established the need to mobilize resources from a variety of financial and technological sources, among other means of implementation.³ For this reason, the UN Department of Economic and Social Affairs published the *Global Sustainable Development Report (GSDR) 2019: The Future is Now – Science for Achieving Sustainable Development*.⁴ In this report, the scientific and technological contributions are defined as the pathway to sustainability transformation and technological innovation to shifting away from the creation of business-as-usual together with the action of scaling up applications of scientific knowledge.⁴ It also identifies science, technology, and innovation as central tools for SDG implementation and explains how technology is usually already available.⁴ Finally, it recommends prioritizing the strategic deployment of novel technologies to minimize the issues to achieve the goals.⁴

Over the past few years, reports have shown how nanostructured materials (or nanomaterials) can make a difference in applications in health and well-being, water treatment and sanitation, and responsible consumption and production of resources. An example is how metal-based nanostructures have been implemented in environmental remediation, electronics, gene therapy, and drug delivery solutions; this is because of their remarkable characteristics, like their higher surface area, surface energy, and chemical reactivity concerning macroscopic materials.⁵ Specifically, bimetallic nanoparticles (BMNPs) have

^aSchool of Engineering and Sciences, Tecnológico de Monterrey, Eugenio Garza Sada 2501, Tecnológico, Monterrey, 64849, NL, Mexico. E-mail: jorgeluis.cholula@tec.mx

^bInstitute for Obesity Research, Tecnológico de Monterrey, Eugenio Garza Sada 2501, Tecnológico, Monterrey, 64849, NL, Mexico

[†] These authors contributed equally.



caught attention lately due to their enhanced features compared to monometallic nanostructures, including improved optical and catalytic properties.^{6,7} Given these reasons, it has been identified that BMNPs can adopt a problem-focused and solution-oriented perspective toward SDGs 3: good health and well-being, SDG 6: clean water and sanitation, and SDG 12: responsible consumption and production.^{8–10}

Although there exist reported studies that imply the use of metallic nanoparticles in the Sustainability Agenda affairs, there are still no review articles that directly link the use of these nanostructures towards accomplishing the SDGs.^{11–14} Taking into account the enhanced properties that BMNPs exhibit towards a wide variety of applications and that nanomaterial-based products have been available in the market since the past decade¹⁵ and the need for more sustainable synthesis methods as well as long-term risks and hazards that these nanomaterials may cause, this review outlines the green synthesis trends of BMNPs whose application aligns with SDGs 3, 6, and 12. We describe the properties and characteristics of the NPs depending on their structure, possible chemical composition, and way of synthesis to indicate their advantages and disadvantages. Furthermore, we present case studies of bimetallic nanostructures synthesized by traditional and green synthesis methods to display their potential application in relation to the mentioned SDGs, highlighting the advantages and feasibility implications of the latest. Finally, we give a perspective on the importance of the synthesis method in relation to the intended applications, together with the metallic NPs positioned in the market and their implications in the sustainability agenda.

2 Properties of metallic nanoparticles

Plasmonic behavior is one of the main enhanced properties that metallic nanostructures manifest.¹⁶ For example, AgNPs can interact with light in different ways depending on their size and structure.¹⁶ When interacting, the incident wavelength of light makes the conduction electrons located in the surroundings of the NP oscillate in an ordered way, generating what is called the localized surface plasmon resonance (LSPR).¹⁷ This phenomenon has been used for electromagnetic enhancement of spectroscopic signals, *e.g.*, surface-enhanced Raman scattering (SERS), which has led to the development of nanostructured systems for detecting chemical and biological molecules.¹⁶ Apart from detection methods, Ag NPs and Au NPs can be used in the biomedical field, specifically in the antibacterial activity towards anticancer therapies.¹⁸ In the work of Soliman *et al.*,¹⁸ results showed that Ag NPs and Au NPs could be further used as active antibacterial, antimicrobial, antibiofilm, antioxidant, and anticancer agents.

Metallic nanostructures are also well-known for their catalytic activity, which can introduce improved performance in the degradation of environmental contaminants. Copper (Cu) is a low-cost and abundant metal;¹⁹ therefore, Cu NPs have been used as promising materials for the degradation of water pollutants like Congo red (CR) and Methylene blue (MB).²⁰ The Cu NPs have shown better catalytic properties in the reduction mechanism of the pollutants compared to NaBH₄, a common

reducing agent, leading to faster and complete removal of CR and MB.²⁰ Apart from the degradation properties, Cu NPs can also reduce CO₂-saturated aqueous solutions at ambient pressure and temperature *via* electrochemical methods.²¹

2.1 Comparison between mono- and bimetallic nanoparticles

Bimetalization strategies lead to materials that combine two different metals exhibiting enhanced and modified properties with respect to a monometallic system. BMNPs have distinctive advantages compared to their monometallic counterparts.¹³ First, bimetalization increases the catalytic properties of the system in comparison to their monometallic counterpart, *i.e.*, monometallic nanoparticles (MNPs).⁷ For instance, electronic transitions in nanowires (NWs) are facilitated with bimetallic systems like Pd–Ni, Pt–Ag, and Pd–Au NWs, which have exhibited desirable stability and a larger surface area, and hence a favorable electrochemical performance.²² Then, the presence of two different metals produces a synergistic effect due to the combination of electronic, mechanical, functional, and structural modifications.⁷ These interactions set off controlled optical, electronic, plasmonic, thermal, and magnetic properties, increasing their functionality and widening their application compared to MNPs.^{23–26} Yang *et al.*¹⁹ investigated the thermal properties of a BMNP-incorporated conductive ink by analyzing its decomposition temperature *via* differential scanning calorimetry (DSC). The results showed that Cu/Ag NPs give the ink a higher decomposition temperature compared to the sole Ag NP-incorporated one by around 30 °C. Apart from this, it was shown that this thermal stability may be controlled in a versatile mode by modifying the Cu : Ag weight ratio. A similar approach was carried out by Anjo and team,²⁷ where the plasmonic and magnetic properties of Fe/Ag NPs synthesized *via* a laser ablation method were tested. As in Yang's work, the Fe : Ag composition ratio was varied, and noticeable differences in their UV-vis spectra were observed. By having a greater Fe : Ag composition ratio, the maximum absorbance wavelength was red-shifted gradually, owing to both the composition of the system and its particle morphology. In the case of magnetic properties, all the prepared samples were found to have a superparamagnetic behavior, but the system corresponding to an Fe₅₀:Ag₅₀ composition ratio showed the optimum (higher) magnetic properties. An Fe–Ag nanosystem was also reported by Malik and colleagues, and the reduction capacity of Fe NPs is combined with the catalytic activity of Ag NPs, which may lead to the catalytic reduction of pollutants like nitroaromatic compounds.²⁴ Therefore, by adding transition metals like Cu and Fe to noble metal-based systems, low-cost solutions with enhanced thermal, plasmonic, magnetic, and catalytic properties may be achieved and systematically modified. Lastly, they show chemical stability and easy functionalization.²² Biomarker detectors, like glucose ones, can acquire an enhanced lower limit of detection (LOD) *via* nanobranched bimetallic structures, like AuCu, which leads to acceptable selectivity and stability.²⁸ Due to these enhanced features, it is expected that BMNPs could signify a more efficient path toward achieving sustainability agenda affairs.



2.2 Structure and characteristics of bimetallic nanoparticles

The structure, architecture, and composition of bimetallic systems play an important role in determining their classification.²⁹ According to the structure, BMNPs are labeled as mixed or segregated (Fig. 1). Mixed structure BMNPs, concomitantly, are classified in two depending on their atomic architecture. On the one hand, if the BMNP has a random configuration of its atom constituents, it is known as an alloy structure²⁹ (Fig. 1A). On the other hand, if its atomic configuration has an ordered pattern, it is known as an intermetallic structure²³ (Fig. 1B). Furthermore, segregated structured BMNPs are composed of two different metals and can have a subcluster or core-shell architecture.²⁹ In the subcluster architecture, or Janus configuration, two different metals have a common interface (Fig. 1C), and in the core-shell BMNP, one metal (core) is surrounded by another metal (shell)²⁹ (Fig. 1D). The metals involved in both structures may be transition and/or noble metals. According to their composition, BMNPs composed of noble metals can exhibit strong plasmon resonances due to their electronic configuration, which is also responsible for their high catalytic properties.³⁰ In addition, the most commonly used metals for bimetallic systems are gold (Au), cobalt (Co), iron (Fe), nickel (Ni), and Ag.²¹ These metals' magnetic and catalytic properties result from their outermost ns electrons and their unsaturated ($n - 1$)d electron shell.²³ Lastly, incorporating transition metals into noble metals reduces the cost of BMNPs as the latter's abundance in the earth's crust is low, and the distribution is dispersed,³¹ making them highly costly.

3 Green synthesis trends of bimetallic nanoparticles

Since Norio Taniguchi coined the term nanotechnology in 1974, this technology has been implemented in new processes, materials, components, and systems, giving new applications in the fields of health care,³⁵ food,³⁶ materials,³⁷ and energy.³⁸ This has impacted our lives and the way we propose innovative solutions to the challenges that the world

is currently facing. In 2005, Barbara Karn, actual co-founder and Executive Director of the Sustainable Nanotechnology Organization (SNO), stated that “*nanotechnology can help with sustainability issues such as climate change, resource depletion, population growth, urbanization, social disintegration, and income inequality*”.¹¹ This statement at that time seemed to link nanotechnology to the term sustainability science, a discipline that aims to direct a sustainable society.¹¹ Nowadays, sustainability science is a field that seeks to understand the fundamental character of interactions between nature and society and to encourage those interactions along more sustainable paths.³⁹ In other words, it is a term for the research community's contributions to addressing the challenges of sustainable development.⁴⁰ According to the Global Sustainable Development Report 2019, the world now needs more sustainability science and proposes two modes of scientific engagement towards the SDG to cover this need.⁴ The first mode, referring to the 2030 Agenda, means to assess the impact of human-environmental dynamics and provide a better understanding of complex causal chains driving the phenomena that affect multiple dimensions of sustainable development.⁴ The second model, labeled guided by the 2030 Agenda, refers to exploring solutions and possible pathways to achieve the SDG.⁴ Based on this last mode, it has been identified that BMNPs can be adapted to the problem-focused and solution-oriented perspective toward SDGs 3, 6, and 12.

Even though chemically synthesized BMNPs have presented favorable results towards SDGs 3, 6, and 12, as presented in Table 1, their safety profile has been limited by toxic chemicals used for their synthesis. For example, sodium borohydride (NaBH_4), a common reducing agent in synthesizing metal NPs,^{41–45} has been classified as harmful if inhaled or absorbed through the skin.⁴⁶ The use of toxic substances in synthesis is relatively common as they generally afford reactions that are either kinetically or thermodynamically favorable.⁴⁷ Even though this may be considered acceptable to obtain high yield percentages or reproducibility in the case of metallic NPs, the chemical transformation in most cases impacts the products' overall toxicity profile and represents a health and environmental hazard.⁴⁸ Attending to these problems, green nanotechnology focuses on using non-hazardous agents for the environment and emphasizing biological raw materials as sources of reagents in the synthesis of nanomaterials.⁴⁹

In general, BMNPs are synthesized by two general approaches, *i.e.*, the top-down and the bottom-up methods.⁵⁰ The first approach is usually achieved through physical methods, and the second by chemical and biological methods.⁵⁰ In the top-down approach, the bulk material is fragmented into nano-sized structures in the presence or absence of a catalyst.⁵¹ In contrast, the bottom-up methods include extending atomic and molecular precursors to the nanoscale.⁵² The chemical synthesis by co-reduction of two ionic species, a bottom-up method, is one of the most commonly used chemical strategies to synthesize noble metal-based BMNPs, while transition metal-based BMNPs are



Fig. 1 Bimetallic nanostructures. (A) Alloy. Reproduced from ref. 32 with permission from MDPI, copyright 2022. (B) Intermetallic. Reproduced from ref. 24 with permission from Elsevier, copyright 2021. (C) Janus. Reproduced from ref. 33 with permission from John Wiley and Sons, copyright 2020. (D) Core-shell. Reproduced from ref. 34 with permission from American Chemical Society, copyright 2007. Green and gray colors indicate different types of metals.



Table 1 Traditionally synthesized bimetallic nanoparticles (T-BMNPs) with potential applications towards SDGs 3, 6, and 12. M1/M2, M1@M2, and M1M2 notations denote alloy, core-shell, and BMNPs with undefined structures, respectively. NS: not specified

NPs	Synthesis method	Size (nm)	Morphology	Application	SDG	References
Pd/Cu	Surfactant-directed aqueous method	3	Nanowires	Quantitative determination of organophosphate pesticides in vegetables and fruits	3	22
Fe/Pd	NaBH ₄ reduction	155	NS	Degradation of soil-sorbed trichloroethylene	3	41
Fe/Ag	NaBH ₄ reduction	80	Spherical	Dechlorination and oxidative degradation of 4-chlorophenol	3	43
FeCu	NaBH ₄ reduction	100	NS	Debromination of 2,2',4,4'-tetrabromodiphenyl ether (BDE-47)	3	26
FeNi						
FePd						
FeAg						
FePt						
FeAu						
Fe/Pd	NaBH ₄ reduction	3–6	Spherical	Dechlorination of excess trichloroethene before aquifer spread	3	42
Fe/Ni						
Fe/Cu						
Fe/Ag						
Ag/Ni	NaBH ₄ reduction	20–25	Quasi-spherical	Reusable catalytic system for efficient reduction of <i>p</i> -nitrophenol to <i>p</i> -aminophenol	3, 12	45
Ag/Cu	NaBH ₄ reduction	NS	NS	Reduction of 4-nitrophenol to 4-amino-phenol	3, 6	44
CuAg	NaBH ₄ reduction	59	Spherical	Reduction of nitrophenols and organic dyes	3, 6	65
CuNi		68				
Cu@Fe	NaBH ₄ reduction	70	Spherical irregular	Removal of cesium from contaminated water	6, 12	66
Ag/Au	NS	9.6	Spherical	Detection of Cr(vi) ions in water	6	30
Fe/Ni	NaBH ₄ reduction	100	Spherical	Antibiotic tetracycline removal	6, 3	67
Ag/Cu	NS	<100	NS	Packaging material for food preservation	12	68
Ag/Cu	NS	<100	NS	Active chicken meat packaging	12	69
Ag/Cu	NS	<100	NS	Active chicken meat packaging	12	70
CuNi	NaBH ₄ reduction	3.9	Spherical	Hydrogen evolution from ammonia borane hydrolysis	12	71

synthesized using thermal decomposition due to the inability of the NPs to crystallize at room temperature.²⁹ The size, shape, and stability of NPs can be adjusted by controlling the thermodynamic and kinetic conditions in the synthesis.⁵³

Green nanotechnology overcomes the main restrictions of traditional physicochemical approaches, integrating the principles of green chemistry to create eco-friendly and safe synthesis processes using biological sources⁴⁹ and to incorporate large-scale manufacturing and industrial use of nanomaterials with less environmental degradation and potential risks of human health hazards.⁵⁵ BMNPs that can be synthesized in an environmentally friendly fashion following a green chemistry approach that incorporates at least three factors: the use of nontoxic capping agents, less hazardous reducing agents, and the selection of environmentally benign solvents.⁵⁶ Thus, applying these green chemistry principles to the synthesis of nanomaterials made possible the emergence of the field of green nanotechnology.⁴⁹ In this sense, the introduction of green nanotechnology to sustainability science in the synthesis and the application of BMNPs have shown effective results towards soil and water contamination as well as an effective antibacterial activity against pathogen bacterial strains in the health sector and food industry.

Bacteria, fungi, plants, algae, and organic waste such as fruit peels and the biomolecules that compose them are biological sources generally used as reducing and stabilizing agents⁵⁷ (Fig. 2). In both bacteria and fungi-mediated synthesis, metallic salts can be reduced in an intracellular or extracellular environment.⁶ Bacteria-mediated green synthesis of BMNPs can generate zero-valence metallic structures, which can be implemented in biomedical and technological applications.⁶ However, fungi-mediated syntheses are preferable to bacteria-mediated ones since the first ones can be used in scaled-up, faster processes.^{58,59} The plant-mediated syntheses of metallic NPs are some of the most commonly used processes. Usually, these processes start with preparing a liquid extract of the plant, which results in a fine powder, which must then be washed and dried before the synthesis.⁶⁰ These reactions are favorable since plant leaves comprise several functional groups and phytochemicals acting as stabilizing and reducing agents.⁶¹ Polyethylene glycol⁶² and starch⁶³ are some of the commonly used materials to achieve a biomolecule-mediated synthesis of metallic NPs. Lastly, waste material-mediated synthesis is one of the less explored types of synthesis.⁶ Nevertheless, its implementation in scale-up processes can highlight circular-economy-based models. Generally, the type of waste used



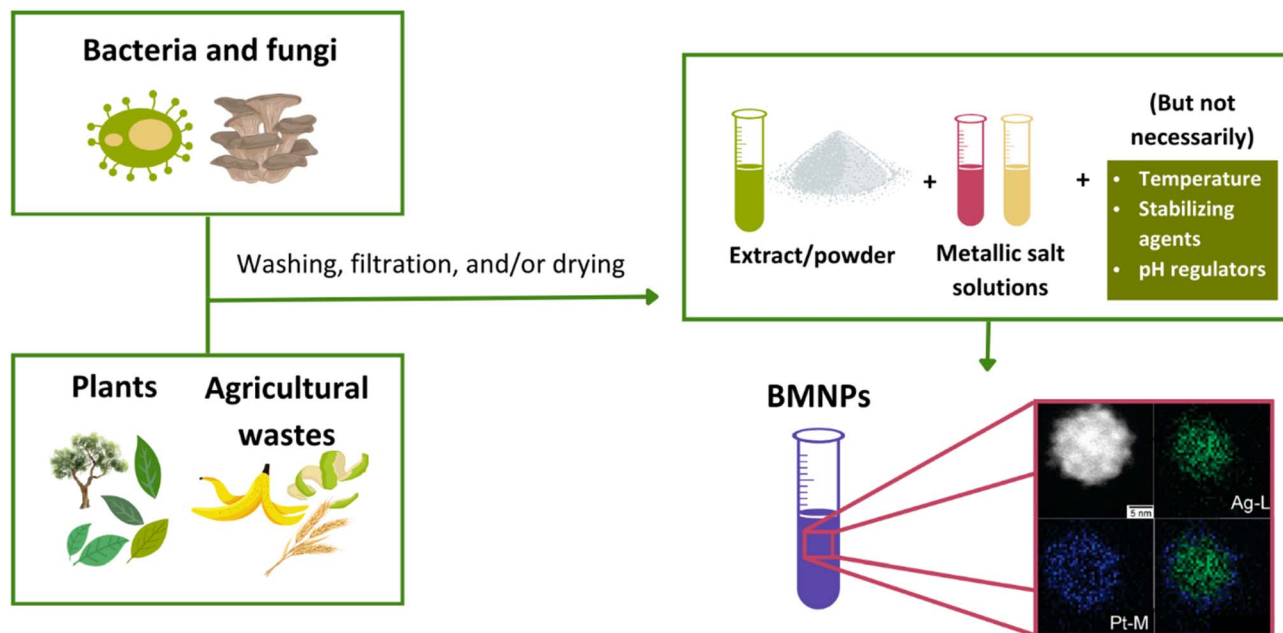


Fig. 2 General methodology for the synthesis of BMNPs via green chemistry methods. Reproduced from ref. 54 with permission from American Chemical Society, copyright 2010.

comes from agricultural wastes, such as fruit peels and organic waste materials. Compared to traditional (also known as “physicochemical”) methods, a remarkable advantage is that green synthesis involves fewer reactants, since, in most cases, reducing and stabilizing agents are the same substance.⁶¹ Furthermore, green nanotechnology presents the advantage of energy efficiency and cost-effectiveness as the synthesis carried out following its principles is low in energy consumption and, consequently, low cost. In addition, they are clean and easy and show a decrease in the production of greenhouse gasses and wastes, as well as a minimal consumption of non-renewable raw materials.^{55,64} BMNPs listed in Table 2 are examples of nanoparticles synthesized by green chemistry methodologies.

The following sections will describe the applications of traditionally and green-synthesized BMNPs (T-BMNPs and G-BMNPs, respectively) towards SDGs 3, 6, and 12. In some cases, one bimetallic nanosystem can be classified into two or more SDGs.

4 Case studies of bimetallic nanoparticles in relation to SDG 3: good health and well-being

SDG 3 prioritizes the assurance of healthy lives and promotes well-being for all ages.⁹⁹ Within the specific targets to achieve this aim, targets 3.3 and 3.9 can be approached by applying BMNPs as a possible solution. On the one hand, target 3.3 aims to end the epidemics of AIDS, tuberculosis, malaria, and neglected tropical diseases, as well as combating hepatitis, water-borne diseases, and other communicable diseases by 2030. Target 3.9, on the other hand, points to substantially

reducing the number of deaths and illnesses produced by hazardous chemicals and contaminants in polluted air, water, and soil.¹⁰⁰ Target 3.9 is important as chemicals used in everyday life goods can greatly affect humans and the environment.¹⁰¹ Fig. 3 summarizes the latest applications of T-BMNPs and G-BMNPs as potential tools for environmental remediation and identification of hazardous chemicals, which will be discussed in the following sections.

4.1 Chemical agent degradation as a pathway for avoiding diseases

Pesticides are one of the types of hazardous chemical agents found in soil. According to recent studies, pesticide pollution is widespread, and its toxicity is a major global health problem.^{102,103} Three million poisoning cases are reported yearly, and between 220 000 and 250 000 deaths occur due to pesticides, where the most common are organophosphates (OPs), specifically malathion.¹⁰³ Given these statistics and the public health concern of pesticide residues in food,^{104–106} Song *et al.*²² developed a highly sensitive, simple, and cost-effective acetylcholinesterase (AChE) electrochemical biosensor for the quantitative determination of malathion in vegetables and fruits based on palladium–copper nanowires (Pd/Cu NWs). The morphology and size of the loaded Pd/Cu NWs on a glass carbon electrode (GCE) showed a high-quality intertwining nanowire morphology with no byproducts such as nanoparticles. The effect of shape control can be attributed to the surfactant-directed aqueous method used to synthesize the bimetallic NWs, as similar shape control results have been reported using this method.¹⁰⁷ Furthermore, according to the results of electrochemical impedance spectroscopy, Pd/Cu NWs could either enhance the conductivity of the electrode interface or facilitate



Table 2 Green synthesized bimetallic nanoparticles (BMNPs) with potential applications towards SDGs 3, 6, and 12. M1/M2, M1@M2, and M1M2 notations denote alloy, core–shell, and undefined BMNPs, respectively

NPs	Synthesis method	Reducing agent	Stabilizing agent	Size (nm) and morphology	Application	SDG	References
Au/Ag	Bioreduction	<i>Barleria prionitis</i> <i>Plumbago zeylanica</i> <i>Syzygium cumini</i>	<i>Barleria prionitis</i> <i>Plumbago zeylanica</i> <i>Syzygium cumini</i>	10–70 not defined 90 hexagonal 10–20 spherical	Antitubercular activity	3	72
Fe/Pd	Bioreduction	Green tea	Green tea	20–100 spherical	Trichloroethylene degradation	3	73
Ir@Cu	Chemical reduction	Ethylene glycol	PVP	1.57 spherical	Congo red dye degradation	3	74
Fe@Ag	Bioreduction	<i>Salvia officinalis</i>	<i>Salvia officinalis</i>	48 spherical	Reduction of the substance 4-nitrophenol	3	24
Au/Ag	Bioreduction	Tannic acid	Tri-sodium citrate	2.9 ± 1.1 spherical	Zika virus RNA detection	3	75
Au@Ag	Bioreduction			4.4 ± 0.6 spherical			
PdCo	Bioreduction	<i>Cinnamomum verum</i>	<i>Cinnamomum verum</i>	2.4 spherical	Dopamine detection and antibacterial activity against <i>S. aureus</i> and <i>E. coli</i>	3	76
AgAu	Bioreduction	<i>Eichhorniacrassipes</i>	<i>Eichhorniacrassipes</i>	0.31–1.08 spherical and cubic	Biosorption of heavy metals (Pb, Zn, Cu, and Mn)	3, 6	77
FeNi	Bioreduction	<i>Pomegranate peel</i>	CMC	129 ± 7 spherical	Antibiotic tetracycline removal	3, 6, 12	78
Fe/Cu	Bioreduction	<i>Pomegranate peel</i>	CMC	60 spherical	Antibiotic tetracycline removal	3, 6, 12	79
Fe@Pd	Bioreduction	<i>Pomegranate peel</i>	CMC	40 spherical	Antibiotic tetracycline removal	3, 6, 12	80
Ag/Cu	Bioreduction	<i>Carica papaya</i>	<i>Carica papaya</i>	150 star-like	Degradation of chlorpyrifos pesticide in water	6	81
Fe/Pd	Bioreduction	<i>Eucalyptus</i>	<i>Eucalyptus</i>	30–60 spherical	Removal of arsenic from natural drinking water	6	82
Cu/Zn	Bioreduction	<i>Hibiscus rosa sinensis</i>	<i>Hibiscus rosa sinensis</i>	Not defined	Antimicrobial activity in hydrocolloid films	12	83
Au/Pt	Microwave-assisted reduction method	Trisodium citrate	—	20–40 spherical, triangle, ellipsoidal	Antibacterial activity against <i>E. coli</i> , <i>S. typhi</i> , <i>Klebsiella</i> , <i>E. coli</i> and <i>E. faecalis</i>	12, 3	84
Ag/Au	Bioreduction	<i>Plumbago zeylanica</i>	<i>Plumbago zeylanica</i>	93 hexagonal and spherical	Antibiofilm activity against <i>E. coli</i> , <i>A. baumannii</i> , <i>S. aureus</i> , and a mixed culture of <i>A. baumannii</i> and <i>S. aureus</i>	12, 3	85
Ag/Au	Bioreduction	<i>Annona squamosa</i> L.	<i>Annona squamosa</i> L.	30–50 diverse	Antibacterial activity against <i>B. subtilis</i> , <i>S. aureus</i> , <i>E. coli</i> and <i>S. typh</i>	12, 3	86
Cu@Pt	Bioreduction	<i>Agrimoniae herba</i>	<i>Agrimoniae herba</i>	30 spherical	Antibacterial activity against <i>E. coli</i> , <i>S. aureus</i> , and <i>P. aeruginosa</i>	12, 3	87
Cu/Au	Bioreduction	<i>Aspergillus niger</i>	—	23–199 triangular	Antimicrobial activity <i>E. coli</i> , <i>K. pneumoniae</i> , <i>P. aeruginosa</i> , <i>P. vulgari</i> , <i>S. aureus</i> , <i>E. faecalis</i> , and fungal strain of <i>A. niger</i> and <i>C. albicans</i>	12, 3	88
Fe/Mn	Bioreduction	Auxin complex (indole-3-acetic)	Auxin complex (indole-3-acetic)	250–300 spherical	Plant bio-fertilizer	12	89
Pt@Ag	Bioreduction	<i>Hibiscus sabdaridha</i>	<i>Hibiscus sabdaridha</i>	5–6 spherical	Hydrogen evolution and antibacterial activity	12, 3	90
Pd–Ag	Bioreduction	<i>Nigella Sativa</i>	<i>Nigella Sativa</i>	6–7 spherical	Hydrogen production, antibacterial and anticancer activities	12, 3	91
Pt–Ag	Bioreduction	<i>Nigella Sativa</i>	<i>Nigella Sativa</i>	5–6 spherical	Hydrogen production, antibacterial activity and photodegradation of azo dyes	12, 6, 3	92



Table 2 (Contd.)

NPs	Synthesis method	Reducing agent	Stabilizing agent	Size (nm) and morphology	Application	SDG	References
PdPt	Bioreduction	<i>Nigella Sativa</i>	<i>Nigella Sativa</i>	10–25 spherical	Hydrogen production, antibacterial and anticancer activities	12, 3	93
Pd–Ag	Bioreduction	Stevia extract	Stevia extract	5–15 spherical	Hydrogen production and antibacterial activity	12, 3	94
Fe–Cr	Coprecipitation with simulated industrial effluents	—	—	20 spherical	Ferromagnetic activity for smart material applications	12	95
Ag/Cu	Chemical reduction	Ascorbic acid	Chitosan	50–80 spherical	Antibacterial activity against <i>E. Coli</i> , <i>P. aeruginosa</i> and <i>S. typhi</i>	12	96
Au–Pt	Bioreduction	<i>Pleurotus florida</i>	<i>Pleurotus florida</i>	16 icosahedral	Agro-waste management and anticancer activity	12, 3	97
Fe–Zn	Bioreduction	<i>Citrus limon</i> (L.) <i>Burm. f.</i> wastes	<i>Citrus limon</i> (L.) <i>Burm. f.</i> wastes	126 spherical	Decolorization of reactive-red 2 (RR2) dye	12, 6	98

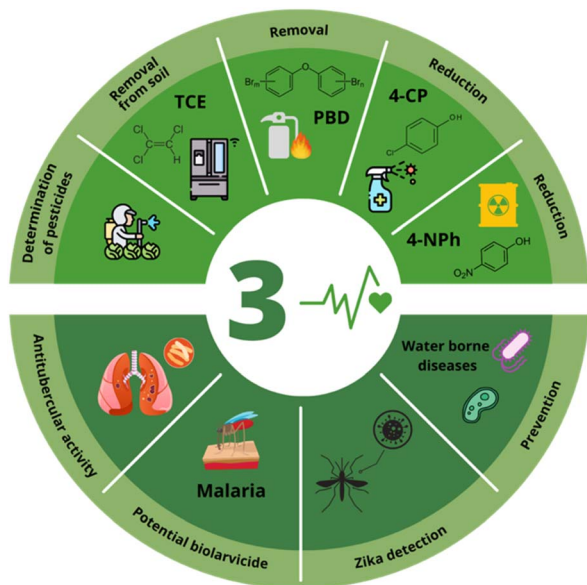


Fig. 3 Applications of traditional and green synthesized BMNPs related to SDG 3: good health and well-being.

electron transfer, as was also reported by Hasanjani and Zarei.¹⁰⁸ Additionally, bimetallic NWs increased the electroactive surface area compared to the bare GCE. Finally, the biosensor indicated an acceptable reproducibility, and its limit of detection (LOD) was estimated to be 1.5 parts per trillion (ppt). This result was lower than the European maximum residue levels of malathion for courgettes, carrots, lettuces, and oranges as well as those obtained by Liquid Chromatography–Mass Spectroscopy method, in which pesticides at concentrations lower than 1.4 part per billion (ppb) cannot be detected.²² These results show that BMNP-based biosensors can potentially be used to comply with pesticide regulations protecting food consumers.

One of the most persistent synthetic phenols used as pesticides or herbicides is a group of chemicals produced by

electrophilic halogenation of phenol with chlorine called chlorophenols.¹⁰⁹ Barreto-Rodrigues *et al.*⁴³ prepared BMNPs of Fe and Ag immobilized in calcium alginate beads (Fe/Ag-Alg) to test dechlorination and oxidative degradation of 4-chlorophenol (4-CP). Batchwise experiments showed that Fe/Ag-Alg completely removed 4-CP under acidic conditions (pH 3). At low pH, BMNPs displayed a low removal of total organic carbon (TOC), which can be explained as the dechlorination process does not allow further degradation, and the reaction products, such as phenols, still need additional treatment. It also presented low Fe leaching compared to bare Fe/Ag. This demonstrates the stability and effective immobilization of Fe/Ag NPs in alginate. Under the same conditions, H₂O₂ was added after dechlorination by Fe/Ag-Alg to increase the TOC removal. Results indicated that adding H₂O₂ completely removed 4-CP and TOC with a relatively low Fe leaching. The results obtained are important as TOC reflects water quality, and according to trials, reducing TOC decreases the formation of carcinogenic compounds such as trihalomethanes (THM).¹¹⁰

Tuberculosis (TB) is caused by *Mycobacterium tuberculosis* and affects millions of people every year.¹¹¹ The resistance of *M. tuberculosis* strains to the four first-line drugs, such as rifampicin, isoniazid, pyrazinamide, and ethambutol, has become a worldwide problem.¹¹¹ Singh and coworkers reported the synthesis of Au/Ag NPs mediated by three different medicinal plants as reducing agents (*B. prionitis*, *P. zeylanica*, and *S. cumini*) and the evaluation of their antitubercular activity.⁷² Results from preliminary screening assays showed that the three bimetallic nanosystems inhibited mycobacterial growth by 90%, indicating that BMNPs have a profound mycobactericidal potency. Moreover, *in vivo* and *ex vivo* macrophage infection assays showed that *S. cumini*-Au/Ag NPs effectively inhibit both active and dormant mycobacteria at a low minimum inhibitory concentration (MIC) and had a greater specificity towards mycobacteria in contrast with the host cells. Although the result did not show rifampicin's high selectivity, Au/Ag NPs can be used as an attractive strategy to overcome rifampicin drug resistance and treat tuberculosis.⁷² Gopinath



*et al.*¹¹² also synthesized Au/Ag NPs using *Terminalia arjuna* as a reducing agent to control the malaria vector *Anopheles stephensi*. In the larvicidal bioassay, Au/Ag NPs showed a higher susceptibility rate in contrast with individual Ag or Au NPs. Therefore, it was concluded that phyto-mediated synthesized metal NPs could potentially be used to control malaria transmission, diminishing long-term undesirable effects produced by synthetic insecticides.¹¹²

4.2 Targeting human exposure to soil pollutants

Retaking the soil pollution approach, trichloroethylene (TCE) is another health-alarming soil chemical pollutant. TCE is an organic compound with low water solubility and one of the most widely chlorinated hydrocarbons used in industry.¹¹³ From its whole annual production, it is estimated that 83.60% of the TCE's annual production volume is used as an intermediate in the manufacture of hydrofluorocarbon HFC-134a,¹¹⁴ which is primarily used as a refrigerant for domestic refrigeration and automobile air conditioners.^{114,115} TCE's low solubility and high absorbance by soil organic matter (SOM) may produce a water/soil distribution, leading to environmental contamination with human health implications.¹¹⁴ According to Dumas, chronic TCE exposure through industrial operations or contaminated drinking water can affect vital organs such as the liver and kidneys.¹¹³ Dechlorination of TCE using BMNPs has been proposed as a remediation strategy to diminish its environmental impact on contaminated soil and groundwater.^{41,116,117} FePd NPs stabilized with carboxymethyl cellulose (CMC) have been used to perform TCE *in situ* dechlorination.^{41,116} Zhang *et al.* studied the reactivity of BMNPs, testing TCE degradation by spherical FePd NPs stabilized with 0.2% CMC.⁴¹ Degradation results showed that after 40 min BMNPs led to the destruction of nearly all the initial TCE. One of the critical aspects during the reaction of TCE degradation is the production of toxic intermediates. Nevertheless, the mass balance of the presented FePd NPs indicated rapid and nearly complete TCE dechlorination without the presence of vinyl chloride and dichloroethenes as by-products. Besides, CMC monodentate interaction with FePd NPs suppressed the growth of nanoparticles, maintaining a higher surface area, provided stability against aggregation in water, and allowed NPs to pass through and be thoroughly dispersed in the soil bed, in contrast to non-stabilized FePd NPs, which were retained on the top of the soil bed. These results were obtained in the presence of a surfactant, and the evaluation of its activity was held in two different soil matrices, and they were comparable with the ones obtained by He *et al.*⁴²

The TCE degradation properties of BMNPs were also tested by Smuleac *et al.*,⁷³ following a green synthesis method. In this study, bimetallic Fe/Pd NPs were immobilized in a polyacrylic acid, PAA-coated polyvinylidene fluoride membrane. First, Fe NPs were loaded into the polymeric membrane, immersing it into an FeCl₂ solution, which functioned as the precursor salt. The reducing and capping agent utilized for the synthesis was a green tea extract, which has proved to contain polyphenols in a concentration that makes it suitable for the synthesis. After

the Fe²⁺ modified membrane was prepared, it was immersed in the green tea extract solution. The third and last step after synthesizing the Fe NPs within the membrane was another process of immersion, this time in a K₂PdCl₄ solution, for the loading of Pd into the Fe NPs. For the TCE degradation performance study, small pieces of the membrane were cut and immersed into a TCE solution. Studies were carried out first with a membrane that contained only Fe NPs, and then with the BMNP membrane. The Fe/Pd-based system showed an increase of its k_{SA} from 0.005 to 0.008 L m⁻², reducing the concentration of TCE to almost 35% of the original concentration, while the solely Fe loaded membrane reduced it to around 60%. The study demonstrated how the bimetalization of NPs can lead to higher degradation activity of TCE. These results are important due to the increasing demand for industrial refrigeration systems across the fast-moving consumer goods sector¹¹⁸ and, as a consequence, the use of TCE.

4.3 Treating industrial wastes

Other persistent organic pollutants in the environment are polybrominated diphenyl ethers (PBDEs). PBDEs are toxic halogenated aromatic compounds used in different industries that generally lack safety precautions in their management and disposal.¹¹⁹ In addition, its high potential for long-range environmental transport can easily produce bio-accumulation in food chains, generating critical adverse health effects in different sectors of the population.¹²⁰ Wang *et al.*²⁶ studied the debromination mechanism of 2,2',4,4'-tetrabromodiphenyl ether (BDE-47) by six different bimetallic systems Fe/M (M: Cu, Ni, Pd, Ag, Pt, and Au). The first important factor they identified was that all the metal additive powders were unreactive toward BDE-47 in the absence of Fe. Therefore, the strong reductive capability of Fe is the primary source of these systems' enhanced activity. Second, the debromination rates of BDE-47 in all the bimetallic systems at the same concentration of metal additive decreased in the following order: Fe/Pd > Fe/Ag > Fe/Cu > Fe/Ni > Fe/Au > Fe/Pt ≈ *n*-ZVI. Third and last, debromination pathways are different for each system. Fe/Ni, Fe/Pd, and Fe/Pt systems have an H-transfer dominant mechanism and generate BDE-17 as the final product. The Fe/Ag system follows an electron-transfer dominant mechanism with BDE-28 as the final product. Finally, Fe/Cu and Fe/Au systems presented a combination of the two mechanisms generating BDE-17 and BDE-28 as final products. This work contributed to understanding debromination and proposed a solution for PBDE pollution to promote well-being. Important to mention is that pre- or post-natal exposure to PBDEs may cause long-lasting behavioral abnormalities, particularly in motor activity and cognition.¹²¹ Apart from PBDEs, synthetic phenols are persistent chemicals that show toxicity.¹²⁰ An example of this is the study performed by Yang *et al.*,¹²² who found that the exposure of zebrafish to synthetic phenolic antioxidants in a range concentration between 5 and 200 μM produced morphological deformities and abnormal pigmentation in their bodies.

The reduction of nitroaromatic (NA) compounds, another type of industrial waste pollutant, can be performed by BMNPs. For



instance, Antony *et al.*⁴⁵ and Zhang *et al.*⁴⁴ proposed the preparation of nanocomposites to reduce nitrophenols (NPh). In the work of Antony *et al.*, a recoverable and reusable catalyst was prepared.⁴⁵ The composite was made of Ag/Ni NPs anchored to a core-shell structure Fe₃O₄@chitosan (CS) as a magnetic support (Fe₃O₄@CS-Ag/Ni). The heterogeneous catalyst in the presence of NaBH₄ turned the yellow solution of *p*-nitrophenol into a colorless solution, confirming the thermodynamically favorable *p*-nitrophenol reduction. Additionally, the reaction at the optimal catalytic dose was performed in less time compared to its monometallic counterpart (Fe₃O₄@CS-Ag), which was attributed to the synergistic effect of BMNPs present because of the changes occurring in the geometric, electronic, and morphological properties of Ag NPs during the formation of BMNPs with Ni. Furthermore, the composite proved to have a high percentage of conversion and selectivity for a considerable range of nitroarene compounds at room temperature in the presence of NaBH₄. Finally, it was observed that amino groups of Fe₃O₄@CS inhibit the leaching of Ag/Ni NPs, maintaining the catalytic activity after seven catalytic runs. Similar leaching inhibition by non-toxic polymers was reported by Barreto-Rodrigues.⁴³ On the other hand, Zhang *et al.*⁴⁴ developed a composite to chelate Ag/Cu NPs (PP-*g*-EDA@Ag/Cu NPs and PP-*g*-DEA@Ag/Cu NPs) using polypropylene (PP) nonwoven fabric grafted with two different organic compounds, ethylenediamine (EDA) and diethylamine (DEA), for the reduction of 4-nitrophenol (4-NPh). EDX mapping results demonstrate that Ag NPs and Cu NPs homogeneously decorate the fiber surface. Batch-type reduction experiments were performed to evaluate the catalytic activity, in which PP-*g*-EDA@Ag/Cu NPs showed a reduction of high concentrations of 4-NPh (1–2 mM) compared to PP-*g*-DEA@Ag/Cu, in which the BMNP load was lower (<1 mM). The observed synergistic effect and adsorption energy corroborated the presence of BMNPs. Moreover, the lack of metal leaching and stability indicated that PP-*g*-EDA@Ag/Cu NPs could be used in dynamic and static catalytic experiments. Ultimately, the evaluation of the composite in tap water showed a catalytic reduction of 98%, and further tests showed that PP-*g*-EDA@Ag/Cu NPs had the potential to treat wastewater with multi-organic substances. Comparable reduction results were obtained by Cu/Ag NPs and Cu/Ni NPs supported on ginger rhizome powder (GP) synthesized by Ismail *et al.*⁶⁵ In this work, Cu/Ni NPs-GP showed less reduction time than Cu/Ag NPs-GP with a high reduction rate for 2-NPh and 4-NPh. Furthermore, the immobilized BMNPs showed catalytic reduction activity towards Methyl orange (MO), Congo red (CR), and rhodamine B (RhB). In the evaluation of the reduction of these dyes, Cu/Ni NPs-GP presented a higher reduction percentage compared to Cu/Ag NPs-GP. Nevertheless, in the reusability assessment, Cu/Ni NPs-GP presented less catalytic activity than Cu/Ag NPs-GP. This is attributed to the fact that Cu/Ni NPs-GP-based catalysts may be oxidized during the reduction process. Furthermore, Cu/Ag NPs-GP presented exceptional catalytic activity after five cycles. Similar reusability was reported for nano-hybrid bimetallic Au/Pd catalysts designed by Wang *et al.*¹²³

Congo red (CR) dye was also successfully oxidized by utilizing Ir@Cu BMNPs in the work of Pooja and Anjali Goel.⁷⁴ Core-shell Ir@Cu BMNPs were synthesized using ethylene glycol (EG) as an effective reducing agent, together with

polyvinylpyrrolidone (PVP) as a stabilizing agent. The obtained BMNPs were found to have a polygonal shape and rough surface morphology with an average size of 1.54 nm. TEM images were used to verify the core-shell structure of Ir@Cu NPs, resulting in an apparent Ir shell monolayer around the Cu core. The oxidative reaction process of CR was carried out using a solution of hexacyanoferrate(III) ((HCF)(III)), a buffer solution, and Ir@Cu NPs. By varying the pH of the buffer solution, it was found that the optimum pH value was 9.0, under which conditions the maximum ionization was achieved. The kinetics study regarding the catalytic effect of the system with respect to the concentration of Ir@Cu NPs revealed that the oxidation reaction of CR was a first-order reaction with respect to the catalyst concentration. In the degradation test using UV-vis spectroscopy, the absorption band at 490 nm disappeared almost completely at a time interval of 3 h. Finally, LC-MS analysis of the products of the RC oxidative reaction resulted in the presence of less toxic organic products, like 2,3-dihydroxybutane dioic acid and 4-amino-3[[4-hydroxyphenyl]azanyl]naphthalene-1-sulphonic acid.

Despite the activity of BMNPs reducing 4-NPh to 4-aminophenol (4-APH), the use of NaBH₄ as a reducing agent in their synthesis method introduces an environmental hazard,⁴⁶ which can be overcome by implementing green methods to synthesize bimetallic systems for this application. Malik *et al.*²⁴ reported green synthesized Fe@Ag nanoparticles using *Salvia officinalis* as a reducing and capping agent to reduce 4-NPh to 4-APH. FTIR spectroscopic analysis showed that the surface of BMNPs is predominantly composed of polyphenols. These compounds protected zero-valent Fe from oxidation and prevented the agglomeration and aggregation of the NPs, maintaining the catalytic properties of Fe@Ag NPs. The percentage of reduction of 4-NPh to 4-APH was close to the results shown when T-BMNP Ag/Cu NPs were used,⁴⁴ as well as their reusability. These characteristics made Fe@Ag NPs an effective green catalyst to reduce 4-NPh, one of the 114 more noxious organic pollutants according to the Environmental Protection Agency (EPA), to 4-APH, which is an intermediate in the synthesis of paracetamol and has important applicability in the textile, leather, and alimentary industries.⁴⁴ Malik *et al.* work is of interest due to an effective reduction of 4-NPh, producing an industrially valued chemical and promoting well-being as localized 4-NPh transformation would eradicate the symptoms generated by its chronic exposure and its genotoxicity.¹²⁴ Continuing this health approach, G-BMNPs have been reported valuable in treating and detecting tuberculosis, malaria, and other illnesses, like the one associated with the Zika virus.

4.4 Health diagnostics

Related to mosquito transmission diseases, the Zika virus (ZIKV) has raised international public health concerns due to its associated symptoms and syndromes. Furthermore, ZIKV diagnostic methods face real challenges as conventional laboratory diagnostics can only record reliable data in the first seven days of the onset of symptoms.⁷⁵ After that time, the only way to obtain



trustable information is by intensive diagnoses. Adegoke *et al.*⁷⁵ built a biosensor probe for ZIKV detection in response to this challenge. To improve the sensitivity and specificity of the biosensor, they conjugated Au/Ag NPs (alloy) and Au@Ag NPs (core-shell) to CdSe/CdS quantum dots (Qdots). Optical properties confirmed the difference between the alloyed and core-shell NPs. Au@Ag NPs showed two LSPR bands in the UV/vis absorption spectra corresponding to the individual contributions of Ag and Au. In contrast, Au/Ag NPs displayed a single LSPR band. Furthermore, Au@Ag NP-Qdots presented higher colloidal stability than their alloy counterpart. However, Au/Ag NP-Qdots presented a lower LOD than Au@AgNP-Qdots. In the end, the LSPR mediated fluorescence signal was stronger for the bimetallic plasmonic NP-Qdots than that of the single metallic plasmonic NP-Qdots, providing a reliable platform for ZIKV detection.⁷⁵

Dopamine (DA) is a neurotransmitter involved in the signal exchange within the nervous system.⁷⁶ Because of the importance of DA in synaptic processes and nervous diseases, Ameen and colleagues⁷⁶ developed activated carbon (AC) supported palladium cobalt BMNPs (PdCo@AC NPs) following a green synthesis procedure, which was proposed to function as a biosensor of DA. The synthesis was performed using a *C. Verum* plant extract during the reaction, using PdCl₂ and CoCl₂ as precursors. Since the proposed biosensor was based on electrocatalytic sensing, cyclic voltammetry (CV) and differential pulse voltammetry (DPV) were performed to determine the electrochemical behavior of PdCo@AC NPs. In cyclic voltammetry, the materials exhibited high sensitivity and selectivity of the biosensor against DA since an increase in the concentration of DA followed an increase in the current, demonstrating a linear behavior. The same trend was observed in the DPV studies. LOD and LQD values were found to be 5.68 pM and 17.21 pM, respectively. Apart from the biosensing properties of PdCo@AC NPs, the antibacterial activity was tested using Gram positive (*S. aureus*) and Gram negative (*E. coli*) bacteria, where results showed that the BMNPs' strong inhibition properties increased with the increase of NP concentrations. The study showed that, as Ag@Au NPs, green synthesized PdCo@AC NPs provide enhanced features to detection systems.

As mentioned before, target 3.3 aims to eradicate waterborne diseases, which are caused by viruses and bacteria that are ingested through contaminated water, food, or by coming in contact with feces. Two of the most common bacteria related to waterborne diseases are *Escherichia coli* (*E. coli*) and *Salmonella typhi* (*S. typhi*). It has been detected that these two waterborne diseases can be prevented by green synthesized BMNPs.^{75,85–88,125} These bimetallic nanosystems will be detailed in Section 6 where SDG 12 is discussed due to their closer relation to this goal.

5 Case studies of bimetallic nanoparticles in relation to SDG 6: clean water and sanitation

According to van Vliet *et al.*, water scarcity refers to the lack of water in quantity and the deficit of water quality.¹²⁶ Their study shows that currently, the world's population suffers from severe



Fig. 4 Applications of traditional and green synthesized BMNPs related to SDG 6: clean water and sanitation.

water scarcity from an annual average of 40%, taking into account both water quantity and quality.¹²⁶ Aware of the worldwide population's strong demand for clean water, the UN defined SDG 6 as water and sanitation.¹²⁷ SDG 6 seeks to ensure safe drinking water and sanitation for all by implementing sustainable management of water resources, wastewater, and ecosystems and acknowledging the importance of an enabling environment.¹²⁶ Fig. 4 represents the schematic view of some of the applications for traditionally and green synthesized BMNPs related to this SDG, which will be discussed in this section as a possible solution to improve water quality to achieve SDG 6.

5.1 Removing heavy metals from water bodies

Radioactive cesium (Cs) and chromium (Cr) are undesirable metals found in wastewater industrial systems.^{128,129} Given this and looking for a solution toward the release of Cs derived from the accident at the Fukushima Daiichi Nuclear Power Plant, Shubair *et al.*⁶⁶ synthesized Fe NPs and Cu@Fe BMNPs for Cs removal from aqueous solutions. Sorption batch studies showed that the Cu@Fe BMNP sorption process was kinetically faster than that of monometallic Fe NPs. Furthermore, at low concentrations, Cu@Fe NPs presented higher values of maximum removal of Cs, which can be attributed to Cu coating. The presence of Cu increases the surface area and decreases the aggregation and agglomeration of Fe NPs as it also prevents Fe from oxidation by O₂, increasing their reactivity. In a matrix effect evaluation, it was observed that cation ions could block the electron transfer from nanoparticle cores, affecting Cs removal. Nevertheless, it was also observed that Cu@Fe BMNPs selectively adsorbed Cs in the presence of competing cations (Na⁺, K⁺, Mg²⁺, and Ca²⁺), indicating that Cu@Fe NPs could be used as efficient materials for Cs removal from contaminated water.¹²⁹ Due to its high toxicity and related exposure to health



risks, the EPA has defined 0.1 mg L^{-1} as the maximum acceptable amount of Cr in drinking water.¹³⁰ Due to this, Das *et al.*³⁰ investigated the catalytic properties of AuAg NPs decorated on L-cysteine functionalized reduced graphene oxide (L-Cys-rGO) sheets toward the peroxidase mimic oxidation of 3,3',5,5'-tetramethylbenzidine (TMB) in the presence of hydrogen peroxide (H_2O_2) as an easy detection of Cr(VI) in an aqueous medium. The detection by the colorimetric nanostructured probe was possible as Cr(VI) ions promoted the decomposition of H_2O_2 to $\cdot\text{OH}$ radicals in an acidic medium which enhanced the oxidation of colorless TMB to its blue colored oxidation product (oxTMB). At the end of the evaluation, it was concluded that the colorimetric sensor exhibited excellent sensitivity and selectivity toward detecting Cr(VI) ions with an LOD value of $26.39 \mu\text{M}$. This LOD value was lower than the ones obtained by monometallic nanocomposites Au/L-Cys-rGO and Ag/L-Cys-rGO.

Apart from Cr and Cs, metals like lead (Pb), zinc (Zn), copper (Cu), and manganese (Mn) are found as pollutants in water bodies. Adewoye *et al.*⁷⁷ conducted a study where the aforementioned heavy metals were adsorbed by green synthesized AuAg NPs. Synthesis was mediated by *E. crassipies* plants, using silver nitrate and gold chloride as precursor salts. Samples containing metals were obtained directly from pharmaceutical effluent collected from a Nigerian point of discharge to confirm the adsorption properties and capacity of the synthesized BMNPs. The obtained nanostructured particles were found to be both spherical and cubic-shaped. For the study, different amounts of adsorbent material powders were loaded in the effluent sample (1 mg, 5 mg, and 10 mg). The adsorption tests were carried out using an Inductive Coupled Plasma Atomic Emission Spectroscopy (ICP-OES), quantifying the metal concentration of Pb, Zn, Cu, and Mn before and after the mixing of the effluent and the adsorbent material; mixing was performed for 24, 48, and 72 hours. In general, the adsorption of metallic ions was increased with the contact time for the three studied metals; however, a direct increase of adsorption with respect to adsorbent material concentration in the same amount of time was only found in Cu removal. For Zn removal, 61.13%, 34.39%, and 58.12% ionic concentrations were achieved using 1, 5, and 10 mg of AuAgNPs, respectively. The highest removal efficiency was achieved for Pb, adsorbing 93.37% of its ions with a contact time of 72 h between the sample and 1 mg of AuAg NPs. In the case of manganese, with a contact time of 48 h with the NPs, removal percentages were 51.7%, 19.60%, and 38.05% for 1, 5, and 10 mg of adsorbent material, respectively. The study showed that the size and morphology of bimetallic nanoparticles as adsorbent materials are directly linked to their rate and removal capacity of metallic wastes in water. Apart from this, the recuperation of these nanostructured materials should be further studied to make them feasible in real-life applications.

5.2 Pharmaceutical waste degradation

Moving on to the degradation of chemical compounds in water, it has been detected that antibiotics from different sources have

been released into nature, leaving an important environmental footprint.^{131–133} According to Dong *et al.*,⁶⁷ one of the most commonly detected antibiotics in the environment is tetracycline (TC). They reported the synthesis of FeNi NPs to remove TC under various water conditions. Their results showed that FeNi NPs were efficient materials for TC removal, following adsorption and degradation mechanisms. Furthermore, it was confirmed that these mechanisms were associated with the active sites of FeNi NPs and that the stability of the NPs in dispersion was due to electrostatic repulsion providing many available sites, resulting in a fast decrease of TC at the beginning of the degradation process for relatively low concentrations of TC, 50 and 100 mg L^{-1} .

In this view, Ravikumar *et al.*⁷⁸ synthesized FeNi NPs by a green synthesis method and reported similar outcomes to Dong *et al.*⁶⁷ Both FeNi bimetallic systems showed a spherical shape, a size between 100 and 130 nm and removed TC by adsorption and degradation mechanisms. Ravikumar *et al.* showed that a *Pomegranate* extract could substitute NaBH_4 as a reducing agent for this nanosystem. Another advantage was that the green synthesized bimetallic system was coated with carboxymethyl cellulose (CMC), which led to a better dispersion at higher pH values compared to the traditionally synthesized FeNi bimetallic system.^{67,78} Moreover, Ravikumar *et al.* evaluated TC removal in three different matrices and found that the lake water matrix presented the lowest percentage of TC reduction, followed by ground and distilled deionized water matrices. Additionally, they studied the residual toxicity of TC by-products after interacting with FeNi NPs. Viability results showed that TC byproducts had less environmental toxicity than TC without BMNP interaction.⁷⁸ A similar approach was reported by Gopal *et al.*, who also used *Pomegranate* peel to synthesize FeCu⁷⁹ and Fe@Pd⁸⁰ bimetallic systems and their respective composites using bentonite (Bt) as supporting materials (Bt-FeCu NPs and Bt-Fe@Pd NPs) for antibiotic TC remediation. In both cases, bentonite composites presented a higher degree of TC reduction than pure bimetallic systems. This behavior is due to bentonite acting as a supporting material and effectively decreasing the aggregation of BMNPs and, consequently, keeping a relatively high surface area. Furthermore, both composites possessed higher stability than BMNPs for prolonged times. In view of these results, the evaluation of pH, residual toxicity, and matrix effects was performed for Bt-FeCu NPs and Bt-Fe@Pd NPs. Experimental results showed the two composites presented approximately the same range of TC effective degradation at both acidic and neutral pH. Nevertheless, a large amount of Bt-Fe@Pd NPs was necessary to achieve this activity compared to Bt-FeCu NPs. Moreover, the outcomes of residual toxicity and removal studies suggested the environmental safety and efficacy of Bt-FeCu NPs and Bt-Fe@Pd NPs for antibiotic removal. Finally, from TC removal studies on different natural water systems, composite Bt-FeCu NPs showed a greater removal in lake water and Bt-Fe@Pd NPs in groundwater. This indicates their potential use towards TC environmental pollution.



5.3 Pesticide removal from water

As mentioned previously, pesticide pollution is considered a global health problem. The spread of pesticides in soil and water systems concerns the scientific community and international organizations. In this regard, the EPA implemented regulations to protect the consumption of drinking water with pesticide contamination.¹³⁴ In view of this, Rosbero and Camacho⁸¹ synthesized star-like Ag/Cu NPs by a co-reduction method using aqueous leaf extracts of *Carica papaya* for water purification applications to degrade chlorpyrifos pesticide. The results of pesticide degradation showed that the star-like Ag/Cu NPs converted chlorpyrifos to less toxic and non-mutagenic degradation products, such as 3,5,6-trichloropyridinol (TCP) and diethylthiophosphate (DETP). Conclusively, using G-BMNPs for chlorpyrifos degradation could be considered a sustainable environmental remediation since it can be applied at room temperature without the need for UV light activation.⁸¹ Furthermore, arsenic (As) is one of the compounds present in pesticides. Lin *et al.*⁸² synthesized calcined Fe/Pd NPs for As(III) removal from wastewater. Calcination caused an increase in the specific surface area, which provided additional active adsorption sites for both As(III) and As(V). Furthermore, it was observed that an alkaline pH and a higher adsorbent dose improved the removal efficiency of As(III). In this study, calcined-Fe/Pd NPs provided a complete removal (100%), proving to be a suitable composite for As removal from wastewater.

Some previously described studies embark on water and sanitation and contribute to achieving SDG 12: responsible consumption and production.^{128,131} This is important as the current lifestyles do not involve responsible consumption and production patterns. Due to the relevance of this sustainable goal, specific examples of BMNPs related to SDG 12 are going to be discussed in the following section.

6 Case studies of bimetallic nanoparticles in relation to SDG 12: responsible consumption and production

It has been detected that one of the main causes of food loss is microbiological food spoilage, which impacts food quality and shelf life. Food spoilage results from microbiological, chemical, or physical changes in food products, making them unsuitable for consumption.¹³⁵ These issues may result in a variety of infections and/or intoxications for consumers.¹³⁶ Additionally, the UN reported that each year, approximately 1.3 billion tons of all food produced worldwide is lost or wasted. Concerned by these undesirable consumption and production patterns, SDG 12.3 stated the goal to halve per capita global food waste at the retail and consumer levels and reduce food losses along production and supply chains, including post-harvest losses by 2030.¹³⁷ In the face of this problem, BMNPs synthesized by traditional and green synthesis methods could be taken as a strategy to increase the shelf life, avoiding food loss. Some of

these solutions are shown in Fig. 5 and are discussed in the following section.

6.1 Packaging solutions

It is estimated that around 20–60% of fresh food production suffers losses at various operational levels in the supply chains.¹³⁸ Attending this, recent studies have focused on designing and creating food packaging films to avoid losses in the production chain. A case in point is the work of Arfat *et al.*, who synthesized three different nanocomposite films using agar,⁶⁸ polylactide (PLA)⁶⁹ and linear low-density polyethylene (LLDPE)⁷⁰ as polymeric matrices and loaded them with Ag/Cu NPs (Ag/Cu NPs-agar, Ag/Cu NPs-PLA, and Ag/Cu NPs-LLDPE, respectively). In the case of Ag/Cu NPs-PLA and Ag/Cu NPs-LLDPE composites, cinnamon essential oil was loaded together with BMNPs. The results showed that adding NPs caused a change in film opacity, impeding the transmission of UV and visible light through the films. These changes in the color parameters were attributed to the surface plasmon resonance of the Ag/Cu NPs, making the composite films feasible as packaging for easily-oxidizing food due to light radiation. Furthermore, the three composites improved the oxygen barrier properties and antimicrobial activity, which could be explained by the release of Ag⁺ and Cu²⁺ ions into the bacterial membrane and their interaction with enzymes and organelles, producing cellular death. To corroborate the antibacterial activity in real samples, microbial validation tests were performed in chicken samples for Ag/Cu NPs-PLA and Ag/Cu NPs-LLDPE composites. Both exhibited remarkable growth reduction against *Listeria monocytogenes* (*L. monocytogenes*), *Salmonella Typhimurium* (*S. Typhimurium*), and *Campylobacter jejuni* (*C. jejuni*). From these three, the nanocomposites showed the greatest bacterial

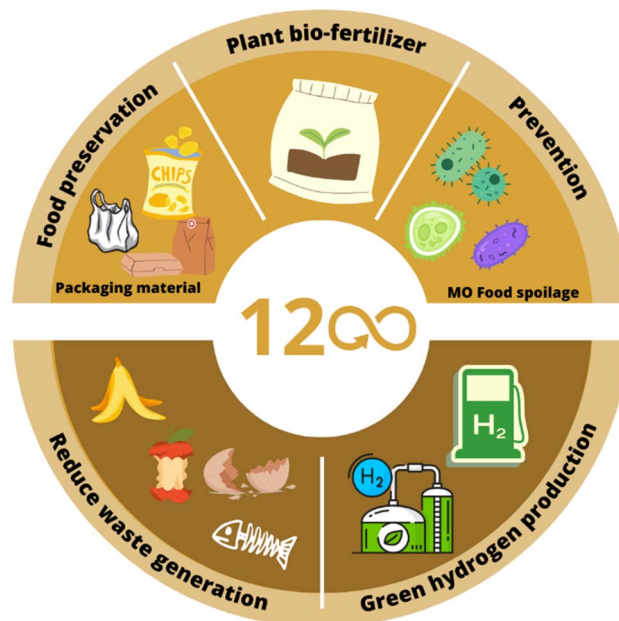


Fig. 5 Applications of traditional and green synthesized BMNPs related to SDG 12: responsible consumption and production.



inhibition against *S. Typhimurium* and *C. jejuni*, indicating antimicrobial effectiveness against Gram-negative bacterial strains over Gram-positive microorganisms. Overall, the three nanocomposite films exhibited the potential to act as an antimicrobial packaging material to inhibit the development of *S. typhimurium* as a foodborne pathogen. These results are of great interest as *S. typhimurium* and other foodborne pathogens, such as *E. coli*, cause post-harvest losses of fruit.¹³⁹

Targeting the same food packaging aspect with a green synthesis approach, Singh synthesized Zn/Cu BMNPs using *Hibiscus rosa sinensis* flower (HRS-F) extract as a reducing, stabilizing, and capping agent.⁸³ These synthesized BMNPs were then loaded into a chitosan (1.5 wt%) + pectin (0.5 wt%) hydrocolloid, a commonly used packaging material, for its further test in antimicrobial activity. FESEM analysis of the synthesized Zn/Cu BMNPs showed a rough surface morphology without any sign of agglomeration, exhibiting HRS-Fs' capacity as a good capping agent in the wet-reduction synthesis of MNPs. EDX analysis showed that the Zn and Cu were present as oxides in the synthesized BMNPs, while XRD and TGA characterization exhibited high purity, crystalline, and stable structures. In antimicrobial activity tests, Gram-positive (*Bacillus subtilis*) and Gram-negative (*E. coli*) were used as test samples for loading the chitosan/pectin/Zn/Cu nanocomposite and its further evaluation. The nanocomposite showed a remarkable effect against microbial activity and growth. The surface area, morphology, and distribution of the loaded Zn/Cu BMNPs gave the hydrogel the capacity to interact with the cell's functional groups, which led to killing the analyzed bacteria samples. The loading of the green synthesized BMNPs in the hydrocolloid system was found to be a potential enhancer of the antimicrobial activity for food packaging and films, which could, in the long term, avoid food losses in the chain of supply.

6.2 Food deterioration prevention

According to the FAO, 22% of the fruits and vegetables are lost from post-harvest up to retail,¹⁴⁰ where most losses are due to microbiological and physiological deterioration.¹³⁹ As mentioned before, microbiological food spoilage is caused by microorganisms' enzymes that lead to undesirable by-products in the food.¹³⁵ An example that worries the FAO is food contamination by the *E. coli* bacterium, as it can produce side effects to food loss such as illness and, in severe cases, even death.¹⁴¹ Yadav *et al.*,⁸⁴ Dobrucka *et al.*,⁸⁷ Salunke *et al.*,⁸⁵ Mirzaei *et al.*¹⁴² and Jain *et al.*⁸⁸ reported the green synthesis of bi- and trimetallic NPs that could contribute to the prevention of *E. coli* infections in the food supply chain. Yadav *et al.* synthesized an Au/Pt BMNP-based nanofluid with a microwave-assisted green chemical method. This study showed that BMNPs dispersed in the fluid medium had greater antimicrobial activity compared to nanofluids with mono-Au NPs. Furthermore, in agar disc inhibition zone analysis, it was observed that bimetallic Au/Pt nanofluids presented the maximum inhibition zone against *Klebsiella*.⁸⁴ Due to frequent sources of foodborne infections, including unpasteurized dairy products and juice,¹⁴¹ the outcomes of this study could be coupled with the work of Salari

et al.,¹⁴³ related to the use of nanofluids in thermal processing operations such as pasteurization.

Salunke *et al.*⁸⁵ synthesized Ag/Au NPs to eradicate the formation of bacterial biofilms, which is a severe concern in the food industry, as pathogens are capable of attaching and growing on food surfaces and surfaces of other processing equipments.¹⁴⁴ The bio-reduced nanocomposite of *P. zeylanica* and Ag/Au NPs showed an *E. coli* biofilm inhibition of approximately 98% and higher antimicrobial activity compared to chemically synthesized Ag/Au NPs towards other bacterial strains.⁸⁵ Moreover, BMNPs reduce the biofilm roughness, indicating good biofilm inhibition and disruption.⁸⁵ These results are important as *P. aeruginosa* can generally be found in high concentrations in everyday food, especially vegetables.¹⁴⁵ Finally, Dobrucka *et al.*⁸⁷ and Jain *et al.*⁸⁸ synthesized BMNPs following environment-friendly procedures and evaluated their antimicrobial activity. On the one hand, Dobrucka *et al.*⁸⁷ synthesized Cu@Pt NPs using a medicinal plant, *Agrimonia eupatoria*. The Cu@Pt nanoparticles exhibited maximum activity against Gram-negative bacteria *E. coli* (ATCC 25922).⁸⁷ With similar results, Jain *et al.* used the cell-free extract of the fungi *Aspergillus niger* to synthesize low-cost Cu/Au NPs. *In vitro*, antimicrobial assessment showed that these BMNPs had significant antibacterial activity against *E. coli* (urinary tract infection (UTI) sample) at low concentrations.⁸⁸

In addition to the loss from post-harvest up to the retail, along the farm-to-fork chain, 30% of food is estimated to be lost at the farm level.¹⁴⁶ Towards this challenge, nanotechnology is being adopted in precision farming. An example is the work of Bettencourt *et al.*,⁸⁹ who developed a green synthesized bimetallic Fe/Mn NP-based plant bio-fertilizer. Similarly to Jain *et al.*,⁸⁸ they used a bacteria-fermented supernatant as a reducing agent, establishing an eco-friendly manufacturing technique for this intended use. At the end of the study, it was concluded that Fe/Mn NPs successfully stimulated the growth of maize seedlings.

6.3 Green hydrogen production

In recent years, green hydrogen production has been positioned as one of the most promising alternative energy sources since its global market is expected to increase by 50 million tons in 2024.¹⁴⁷ Nowadays, hydrogen can be produced by four methods: brown, grey, blue, and green production. The first three of these methods come along with high CO₂ emissions; in contrast, green hydrogen production comprises potentially zero net emissions since the splitting of water into hydrogen and oxygen, electrolysis, is powered by renewable energy sources.¹⁴⁷ Usually, electrolysis processes are promoted *via* the utilization of catalysts; therefore, BMNPs have been positioned as effective catalytic agents for these types of applications.⁹¹ In most hydrogen obtention and storage studies, boron hydrides and ammonium borane derivatives are used as hydrogen sources.⁹⁰ For instance, NaBH₄ is a common boron hydride used in the production of hydrogen because it shows a stable performance in alkaline environments and has a high hydrogen density.^{90,91}

In the work of Jiang *et al.*,⁷¹ CuNi NPs were immobilized in a graphitic carbon nitride (g-C₃N₄) network to test its catalytic



activity for hydrogen evolution using ammonia borane (AB) as a H₂ carrier. After preparing g-C₃N₄, it was mixed with the precursor salts of Cu and Ni before adding NaBH₄ to reduce metals and obtain the CuNi-g-C₃N₄ product. SEM and TEM images revealed the porous morphology of g-C₃N₄ and how the Cu Ni NPs, with a mean size of 3.9 nm, were accumulated in the pores. AB hydrolysis was tested with Cu-g-C₃N₄, Ni-g-C₃N₄, and CuNi-g-C₃N₄ catalytic materials. It was found that Ni-g-C₃N₄ was able to produce more H₂ than Cu-g-C₃N₄, showing that Ni is a better booster for H₂ production. However, the bimetallic heterostructure, *i.e.*, CuNi-g-C₃N₄, increased by almost 30 mL the hydrogen production, producing around 75 mL of H₂ and showing how the synergism between Cu and Ni enhanced catalytic activity. Important to mention is that in the case of g-C₃N₄, it was found that it has negligible catalytic activity in an AB environment. Through temperature-dependent tests, it was possible to determine that the activation energy (E_a) of the system was 23.58 kJ mol⁻¹, which is lower than that of many Cu/Ni reported BMNP systems.

In another study, Darabi and colleagues⁹⁰ synthesized Pt@Ag NPs using a *Hibiscus sabdariffa* plant extract. The obtained BMNPs were found to be spherical and with a size of 5 nm, which is comparable to the Pt-Ag NPs synthesized by the team of Gulbaga.⁹¹ In this study, hydrolysis reactions were carried out in an inert atmosphere, using NaBH₄ as the hydrogen precursor. Based on a NP concentration dependency study, it was found that the hydrolysis process comprises a 1st order reaction, showing that the amount of H₂ increases with respect to the concentration of Pt@Ag NPs. The maximum amount of obtained H₂ was around 30 mL, combining 9 mM NPs and 125 mM NaBH₄. The nanocatalysts were found to be effective and recyclable since the calculated reusability between the first and the fifth cycle of hydrolysis was about 85%.

Gulbaga *et al.*⁹¹ fabricated Pd-Ag NPs, with spherical morphology and a particle size around 7 nm, by a green route using a *Nigella Sativa* plant extract. The effects of Pd-Ag NP concentration, temperature, NaBH₄ concentration, and pH of the system were tested towards hydrogen obtention. At a constant NaBH₄ concentration (125 mM), the concentrations of Pd-Ag NPs were 2.25, 4.50, 6.75, and 9 mM, and the process was done for 30 min. Even at the lowest BMNP concentration, the system released around 150% more volume of H₂ than the blank test, *i.e.*, without BMNPs, showing high catalytic activity and better performance compared to the work of Darabi,⁹⁰ producing 10 mL more than the mentioned work. On the other hand, while having a constant Pd-Ag NP concentration and varying NaBH₄ concentrations, the obtained volume of H₂ reached around 30 mL in 30 min, which is around three times more volume than the blank test at the same time. A temperature test showed that the amount of obtained H₂ increased with respect to the system's temperature. This test was also useful to determine the E_a , change in Gibbs energy (ΔG), and change in entropy (ΔS) of the system, which were 24.51, 27.01, and -183.15 kJ mol⁻¹, respectively. In the case of pH studies, it was found that at lower pH values, the yield of H₂ obtention was favored, with an optimum pH value of 2.82. In

terms of reusability, the system could produce H₂ consistently for five cycles, with a preservation of 98% of the production between the first and the last cycle. In another study carried out by Lin *et al.*,⁹² where Pt-Ag NPs were synthesized with the same plant extract, and the catalytic tests were the same as in the work of Gulbaga,⁹¹ and the team reported very similar quantitative results, showing the replicability of using the plant *Nigella Sativa* as a reducing agent.

The same reducing agent (extracts of *Nigella Sativa*) was used by Aygun and colleagues,⁹³ in the synthesis of PdPt NPs. The obtention of the plant extract was followed similarly to the previously mentioned reports. Again, the experiments were based on NP concentration, NaBH₄ concentrations, temperature, and pH as variables for the catalytic studies. This time, it was found that using low concentrations of PdPt NPs, the production of H₂ was increased around 5.7 times. In the temperature-dependent tests, the kinetics of the system were also analyzed. The results showed that the activation energy of the catalyst was 13.96 kJ mol⁻¹, which is significantly lower than that in most of the previous reports where NaBH₄ is used as a hydrogen precursor.⁹³ In the case of the pH-dependent tests, it was observed that, as with Pd-Ag NPs, PdPt NPs also have higher yields of H₂ production in acidic media. The referred reports, apart from showing the effective use of a *Nigella Sativa* plant extract as a reducing agent, show that Pd-based BMNPs are promising materials for catalytic application in the obtention of H₂ as a potential fuel source.

In another strategy, Mallikarjuna and team⁹⁴ synthesized Pd-Ag BMNPs that were combined with rGO, resulting in Pd-Ag/rGO heterostructures. As in the previous examples, the synthesis of the BMNPs was carried out following a green synthesis route, using a stevia leaf extract. TEM images revealed that the spherical Pd-Ag NPs were distributed on the rGO sheets, with particle sizes ranging from 5–15 nm. In this study, water was used instead of NaBH₄ as the hydrogen source, together with methanol as a scavenger agent. Also, the study tested the photocatalytic activity of the synthesized nanostructures using an artificial solar light simulator. The rGO, Pd/rGO, and Pd-Ag/rGO systems were tested, where the sole rGO system produced the lowest yield of H₂ of 620 $\mu\text{mol g}^{-1}$. The presence of Pd/rGO increased this yield to around 2400 $\mu\text{mol g}^{-1}$, while the system with the highest H₂ production yield was provided by the Pd-Ag/rGO heterostructures with around 5800 $\mu\text{mol g}^{-1}$ of produced H₂ due to a relatively higher surface area, lower band gap and lower electron-hole recombination rate.⁹⁴ The yield of H₂ evolution was found to be non-linear between doses of 2.5–10 mg Pd-Ag/rGO since it reached a maximum value of 5802 $\mu\text{mol g}^{-1}$ of H₂ product with 5 mg of Pd-Ag/rGO, which decreased by increasing the mass of Pd-Ag/rGO. The addition of methanol as a scavenger agent was also tested, and it was found that the optimum concentration was around 5% v/v, since, beyond this value, the production of hydrogen decreases because of generated methanol byproducts. Reusability tests were also carried out, where the Pd-Ag/rGO photocatalytic system decreased its performance only slightly after five cycles of use.



signifies a barrier in removing pollutants from contaminated water since the presence of, for example, heavy metals tends to reduce the pH of water.¹⁶⁹ In addition, the recuperation of nanomaterials in water treatment plants remains a significant challenge, as well as residue disposal after the degradation or adsorption of contaminants. The mentioned solutions attending SDG 12 are mainly focused on NP-loaded food packages. Although metallic nanoparticles have shown enhanced antimicrobial activities, human exposure to these materials is a concern. Nanoparticles can penetrate human skin, facilitating their interaction with human cells and tissues, which may lead to potential health risks.¹⁷⁰ Nanomaterials' toxicity has not been completely understood to date, and the extent to which nanoparticle-based products may lead to cellular damage is still unclear.⁵⁰ Nevertheless, a recent study reported by Lomelí-Marroquín *et al.* showed that green synthesized Ag/Au BMNPs, in the same concentrations, may exhibit lower cytotoxic activity against healthy human cells (human dermal fibroblast) than the one against cancerogenic cells (melanoma).¹⁷¹ At the same, the antibacterial activity tests of Ag/Au NPs showed that the minimum inhibitory values (IC₅₀) were lower for BMNPs than those of mono-MNPs (Au), *i.e.*, the IC₅₀ values were 4.92 and 7.02 µg L⁻¹, respectively, against MDR *E. coli*.¹⁷¹ More of these types of studies should be performed and published so a clear evaluation can be done with respect to the advantages and disadvantages of the usage of BMNPs regarding cytotoxic effects.

In order to address the environmental safety and health issues associated with nanomaterials, the National Institute of Occupational Safety and Health (NIOSH) has established the Nanotechnology Research Center (NTRC).¹⁷² The NTRC was established, among other goals, to research, understand, and publish results from toxicologic tests regarding the potential of metallic nanomaterials to have long-term pulmonary effects, such as fibrosis and lung cancer,¹⁷³ while in the case of environmental damage, it has expressed the necessary understanding of environmental fate, exposure, and ecological effects of engineered nanomaterials.¹⁷³ Therefore, safety control studies of metal-based NPs in commercial and industrial products should be performed before implementing sustainability solutions. Usually, nanomaterial waste products are disposed of in the same ways as conventional wastes;¹⁷² therefore, strict regulations and previous disposal treatments should be strictly regulated in order to enable their use as a completely sustainable practice.

With respect to the measurement of the environmental impact of the application of BMNPs, a study reported by Ulucan-Altuntas *et al.*¹⁷⁴ shows the Life Cycle Assessment (LCA) of the production of FeCu *via* traditional methods, *i.e.*, by using NaBH₄ as a reducing agent. LCA shows that around 87% of the synthesis environmental damage for producing FeCu BMNPs comes from using NaBH₄ in the process.¹⁷⁴ The authors of this report stated that “to remove the borohydride reagent from the method, greener synthesis should be used”, since around 1.87 m³ of wastewater with borohydride concentrations were produced by synthesizing 1 kg of BMNPs.¹⁷⁴ Similar results were obtained in the study performed by Visentin *et al.*,¹⁷⁵ where different production processes of metallic NPs were analyzed

and compared. Again, NaBH₄ reduction was found to be the most hazardous process, resulting in major environmental impacts, such as human health, ecosystem quality, climate change, and resources.¹⁷⁵ The study exhibited that the amount of wastewater produced with BH₄ concentrations during the production of Fe NPs was 0.702 m³, which is less than the production of FeCu BMNPs.^{174,175} Although the mentioned studies reflect that removing NaBH₄ may signify a decrease in environmental and health risks, they mainly focus on parameters such as materials, energy, and water consumption during the synthesis process. This tendency has been seen in most LCA performed during the past few decades, excluding the output flows (releases after production) and the end-of-life stages of NPs.¹⁷⁶ Due to the mentioned reasons and the persistent uncertainties, scale-up, reproducibility, application, and bilateral risk aspects regarding end-of life toxicity related environmental impacts of BMNPs, despite being green synthesized, should be considered and further studied.

8 Final remarks

The featured BMNPs can contribute to addressing sustainable development challenges, specifically as a possible solution for SDGs 3, 6, and 12. Relevant results were shown by both traditionally and green-synthesized BMNPs. However, green synthesis presented cost, energy, and safety advantages over traditionally chemically synthesized BMNPs. It can be concluded that there must be more significant efforts to improve the reproducibility in green chemical routes to upscale their production and to have more studies that show the environmental impact of the use of BMNPs to ensure a clear path of their application towards the Sustainable Development Goals 2030.

Author contributions

Mariana Larrañaga-Tapia: conceptualization, writing – original draft, and writing – editing. Benjamín Betancourt-Tovar: writing – editing. Marcelo Videá: writing – review & editing. Marilena Antunes-Ricardo: writing – review & editing and supervision. Jorge L. Cholula-Díaz: writing – review & editing and supervision.

Conflicts of interest

There are no conflicts to declare.

Acknowledgements

The authors thank the School of Engineering and Sciences at Tecnológico de Monterrey for partial funding provided through the Research Chairs of Nutriomics and Emerging Technologies, and Photonics and Quantum Systems.

References

- 1 The 17 Sustainable Development Goals (SDGs), <https://sdgs.un.org/goals>, (accessed November 2023).



- 2 R. D. Mangukiya and D. M. Sklarew, *World Dev. Sustain.*, 2023, **2**, 100058.
- 3 P. P. Walsh, E. Murphy and D. Horan, *Technol. Forecast. Soc. Change*, 2020, **154**, 119957.
- 4 *The Future Is Now: Science for Achieving Sustainable Development (GSDR 2019)*, UNDESA, New York, 2019.
- 5 S. Islam, S. Bairagi and M. R. Kamali, *Chem. Eng. J. Adv.*, 2023, **14**, 100460.
- 6 D. Medina-Cruz, B. Saleh, A. Vernet-Crua, A. Nieto-Argüello, D. Lomelí-Marroquín, L. Y. Vélez-Escamilla, J. L. Cholula-Díaz, J. M. García-Martín and T. Webster, *Bimetallic Nanoparticles for Biomedical Applications: A Review*, 2020.
- 7 M. Blosi, S. Ortelli, A. Costa, M. Dondi, A. Lolli, S. Andreoli, P. Benito and S. Albonetti, *Materials*, 2016, **9**, 550.
- 8 G. Ren, K. Wan, H. Kong, L. Guo, Y. Wang, X. Liu and G. Wei, *Carbohydr. Polym.*, 2023, **305**, 120537.
- 9 N. Kumar, R. Gusain, S. Pandey and S. S. Ray, *Adv. Mater. Interfaces*, 2023, **10**, 2201375.
- 10 B. M. Trinh, B. P. Chang and T. H. Mekonnen, *Prog. Mater. Sci.*, 2023, **133**, 101071.
- 11 A. Wiek, R. W. Foley and D. H. Guston, in *Nanotechnology for Sustainable Development*, ed. M. S. Diallo, N. A. Fromer and M. S. Jhon, Springer International Publishing, Cham, 2014, pp. 371–390.
- 12 P. Shrivastava, V. K. Jain and S. Nagpal, *Environ. Nanotechnol., Monit. Manage.*, 2022, **17**, 100667.
- 13 D. S. Idris and A. Roy, *Crystals*, 2023, **13**, 637.
- 14 M. Nasrollahzadeh, M. Sajjadi, S. Iravani and R. S. Varma, *Nanomaterials*, 2020, **10**, 1784.
- 15 M. E. Vance, T. Kuiken, E. P. Vejerano, S. P. McGinnis, M. F. Hochella and D. R. Hull, *Beilstein J. Nanotechnol.*, 2015, **6**, 1769–1780.
- 16 J. L. Cholula-Díaz, D. Lomelí-Marroquín, B. Pramanick, A. Nieto-Argüello, L. A. Cantú-Castillo and H. Hwang, *Colloids Surf., B*, 2018, **163**, 329–335.
- 17 G. S. Geleta, *Food Chem. Adv.*, 2023, **2**, 100184.
- 18 M. K. Y. Soliman, S. S. Salem, M. Abu-Elghait and M. S. Azab, *Appl. Biochem. Biotechnol.*, 2023, **195**, 1158–1183.
- 19 W. Yang, C. Wang and V. Arrighi, *J. Mater. Sci.: Mater. Electron.*, 2019, **30**, 11607–11618.
- 20 F. A. M. Alahdal, M. T. A. Qashqoosh, Y. K. Manea, R. K. A. Mohammed and S. Naqvi, *Sustainable Mater. Technol.*, 2023, **35**, e00540.
- 21 F. J. V Gomez, G. Chumanov, M. F. Silva and C. D. Garcia, *RSC Adv.*, 2019, **9**, 33657–33663.
- 22 D. Song, Y. Li, X. Lu, M. Sun, H. Liu, G. Yu and F. Gao, *Anal. Chim. Acta*, 2017, **982**, 168–175.
- 23 A. Behera, N. Patra, B. Mittu, S. Padhi and J. Singh, *Multifunct. Hybrid Nanomater. Sustainable Agri-Food Ecosyst.*, 2020, 639–682.
- 24 M. A. Malik, A. A. Alshehri and R. Patel, *J. Mater. Res. Technol.*, 2021, **12**, 455–470.
- 25 R. Rajeev, R. Datta, A. Varghese, Y. N. Sudhakar and L. George, *Microchem. J.*, 2021, **163**, 105910.
- 26 R. Wang, T. Tang, G. Lu, Z. Zheng, K. Huang, H. Li, X. Tao, H. Yin, Z. Shi, Z. Lin, F. Wu and Z. Dang, *Sci. Total Environ.*, 2019, **661**, 18–26.
- 27 L. Anjo, A. Khajehnezhad, A. H. Sari, S. A. Sebt and M. M. Ismail, *Plasmonics*, 2022, **17**, 941–948.
- 28 A. Ngamaroonchote, Y. Sanguansap, T. Wutikhun and K. Karn-orachai, *Microchim. Acta*, 2020, **187**, 559.
- 29 P. Srinoi, Y.-T. Chen, V. Vittur, M. Marquez and T. Lee, *Appl. Sci.*, 2018, **8**, 1106.
- 30 P. Das, P. Borthakur, P. K. Boruah and M. R. Das, *J. Chem. Eng. Data*, 2019, **64**, 4977–4990.
- 31 L. Y. Jiang and L. Na, *Membrane-Based Separations in Metallurgy Principles and Applications*, 2017.
- 32 A. Nieto-Argüello, D. Medina-Cruz, Y. S. Pérez-Ramírez, S. A. Pérez-García, M. A. Velasco-Soto, Z. Jafari, I. De Leon, M. U. González, Y. Huttel, L. Martínez, Á. Mayoral, T. J. Webster, J. M. García-Martín and J. L. Cholula-Díaz, *Nanomaterials*, 2022, **12**, 779.
- 33 K. Loza, M. Heggen and M. Eppele, *Adv. Funct. Mater.*, 2020, **30**, 1909260.
- 34 D. Ferrer, A. Torres-Castro, X. Gao, S. Sepúlveda-Guzmán, U. Ortiz-Méndez and M. José-Yacamán, *Nano Lett.*, 2007, **7**, 1701–1705.
- 35 S. Singh, P. Tripathi, N. Kumar and S. Nara, *Biosens. Bioelectron.*, 2017, **92**, 280–286.
- 36 L. Kuang, B. Burgess, C. L. Cuite, B. J. Tepper and W. K. Hallman, *Food Qual. Prefer.*, 2020, **83**, 103922.
- 37 S. Talebian, T. Rodrigues, J. das Neves, B. Sarmiento, R. Langer and J. Conde, *ACS Nano*, 2021, **15**, 15940–15952.
- 38 K. Ni, Y. Wu, F. Karimi, F. Gulbagca, A. Seyrankaya, E. Esra Altuner, Y. Kocak and F. Sen, *Fuel*, 2023, **341**, 127577.
- 39 R. W. Kates, *Proc. Natl. Acad. Sci. U. S. A.*, 2011, **108**, 19449–19450.
- 40 H. Komiyama and K. Takeuchi, *Sustain. Sci.*, 2006, **1**, 1–6.
- 41 M. Zhang, F. He, D. Zhao and X. Hao, *Water Res.*, 2011, **45**, 2401–2414.
- 42 F. He, Z. Li, S. Shi, W. Xu, H. Sheng, Y. Gu, Y. Jiang and B. Xi, *Environ. Sci. Technol.*, 2018, **52**, 8627–8637.
- 43 M. Barreto-Rodrigues, J. Silveira, P. García-Muñoz and J. J. Rodriguez, *J. Environ. Chem. Eng.*, 2017, **5**, 838–842.
- 44 X. Q. Zhang, R. F. Shen, X. J. Guo, X. Yan, Y. Chen, J. T. Hu and W. zhong Lang, *Chem. Eng. J.*, 2021, **408**, 128018.
- 45 R. Antony, R. Marimuthu and R. Murugavel, *ACS Omega*, 2019, **4**, 9241–9250.
- 46 L. Banfi, E. Narisano, R. Riva, N. Stiasni, M. Hiersemann, T. Yamada and T. Tsubo, *Encyclopedia of Reagents for Organic Synthesis (EROS)*, 2014, pp. 1–13.
- 47 W. Leitner, *Toward Benign Ends*, American Association for the Advancement of Science, 1999.
- 48 P. Raveendran, J. Fu and S. L. Wallen, *J. Am. Chem. Soc.*, 2003, **125**, 13940–13941.
- 49 M. Nasrollahzadeh, M. Sajjadi, S. M. Sajadi and Z. Issaabadi, *Interface Sci. Technol.*, 2019, **28**, 145–198.
- 50 N. Baig, I. Kammakakam, W. Falath and I. Kammakakam, *Mater. Adv.*, 2021, **2**, 1821–1871.
- 51 G. Sharma, A. Kumar, S. Sharma, M. Naushad, R. Prakash Dwivedi, Z. A. ALOthman and G. T. Mola, *J. King Saud Univ., Sci.*, 2019, **31**, 257–269.
- 52 F. A. A. Nugroho, B. Iandolo, J. B. Wagner and C. Langhammer, *ACS Nano*, 2016, **10**, 2871–2879.



- 53 S. Ali, A. S. Sharma, W. Ahmad, M. Zareef, M. M. Hassan, A. Viswadevarayalu, T. Jiao, H. Li and Q. Chen, *Crit. Rev. Anal. Chem.*, 2021, **51**, 454–481.
- 54 Z. Peng, J. Wu and H. Yang, *Chem. Mater.*, 2010, **22**, 1098–1106.
- 55 S. Aithal and P. S. Aithal, *Green and Eco-Friendly Nanotechnology-Concepts and Industrial Prospects*, 2021.
- 56 H. Duan, D. Wang and Y. Li, *Chem. Soc. Rev.*, 2015, **44**, 5778–5792.
- 57 P. Puja and P. Kumar, *Spectrochim. Acta, Part A*, 2019, **211**, 94–99.
- 58 X. Zhao, L. Zhou, M. S. Riaz Rajoka, L. Yan, C. Jiang, D. Shao, J. Zhu, J. Shi, Q. Huang, H. Yang and M. Jin, *Crit. Rev. Biotechnol.*, 2018, **38**, 817–835.
- 59 M. J. Taherzadeh, M. Fox, H. Hjorth and L. Edebo, *Bioresour. Technol.*, 2003, **88**, 167–177.
- 60 S. S. Nayak, G. C. Wadhawa, K. B. Pathade, V. S. Shivankar and N. A. Mirgane, *Plant Sci. Today*, 2021, **8**, 380–385.
- 61 P. Bairwa and V. Devra, *NanoWorld J.*, 2022, **8**, 6–18.
- 62 A. A. Selim, T. M. Sakr and B. M. Essa, *Pharm. Chem. J.*, 2023, **57**, 29–39.
- 63 C. O. Ogidi, O. P. Emmanuel, O. O. Daramola, O. Bamigboye and O. Malomo, *Turkish JAF Sci. Tech.*, 2023, **11**, 227–238.
- 64 S. S. Salem and A. Fouda, *Biol. Trace Elem. Res.*, 2021, **199**, 344–370.
- 65 M. Ismail, M. I. Khan, S. B. Khan, M. A. Khan, K. Akhtar and A. M. Asiri, *J. Mol. Liq.*, 2018, **260**, 78–91.
- 66 T. Shubair, O. Eljamal, A. M. E. Khalil, A. Tahara and N. Matsunaga, *J. Environ. Chem. Eng.*, 2018, **6**, 4253–4264.
- 67 H. Dong, Z. Jiang, C. Zhang, J. Deng, K. Hou, Y. Cheng, L. Zhang and G. Zeng, *J. Colloid Interface Sci.*, 2018, **513**, 117–125.
- 68 Y. A. Arfat, J. Ahmed and H. Jacob, *Carbohydr. Polym.*, 2017, **155**, 382–390.
- 69 J. Ahmed, Y. A. Arfat, A. Bher, M. Mulla, H. Jacob and R. Auras, *J. Food Sci.*, 2018, **83**, 1299–1310.
- 70 J. Ahmed, M. Mulla, Y. A. Arfat, A. Bher, H. Jacob and R. Auras, *LWT*, 2018, **93**, 329–338.
- 71 R. Jiang, M. Yang, J. Meng, P. Zhao, P. Liu and X. Zheng, *Int. J. Hydrogen Energy*, 2023, **48**, 18245–18256.
- 72 R. Singh, L. Nawale, M. Arkile, S. Wadhvani, U. Shedbalkar, S. Chopade, D. Sarkar and B. A. Chopade, *Int. J. Nanomed.*, 2016, **11**, 1889–1897.
- 73 V. Smuleac, R. Varma, S. Sikdar and D. Bhattacharyya, *J. Membr. Sci.*, 2011, **379**, 131–137.
- 74 P. Goel and A. Goel, *Kinet. Catal.*, 2021, **62**, 592–603.
- 75 O. Adegoke, M. Morita, T. Kato, M. Ito, T. Suzuki and E. Y. Park, *Biosens. Bioelectron.*, 2017, **94**, 513–522.
- 76 F. Ameen, H. Karimi-Maleh, R. Darabi, M. Akin, A. Ayati, S. Ayyildiz, M. Bekmezci, R. Bayat and F. Sen, *Environ. Res.*, 2023, **221**, 115287.
- 77 S. O. Adewoye, V. O. Adenigba, A. O. Adewoye and T. A. Adagunodo, *IOP Conf. Ser. Earth Environ. Sci.*, 2021, **655**, 012021.
- 78 K. V. G. Ravikumar, S. V. Sudakaran, K. Ravichandran, M. Pulimi, C. Natarajan and A. Mukherjee, *J. Cleaner Prod.*, 2019, **210**, 767–776.
- 79 G. Gopal, H. Sankar, C. Natarajan and A. Mukherjee, *J. Environ. Manage.*, 2020, **254**, 109812.
- 80 G. Gopal, R. Kvg, M. Salma, J. Lavanya Agnes Angalene, N. Chandrasekaran and A. Mukherjee, *J. Environ. Chem. Eng.*, 2020, **8**, 104126.
- 81 T. M. S. Rosbero and D. H. Camacho, *J. Environ. Chem. Eng.*, 2017, **5**, 2524–2532.
- 82 Y. Lin, X. Jin, N. I. Khan, G. Owens and Z. Chen, *J. Cleaner Prod.*, 2021, **286**, 124987.
- 83 A. K. Singh, *Bioresour. Technol. Rep.*, 2022, **18**, 101034.
- 84 N. Yadav, A. K. Jaiswal, K. K. Dey, V. B. Yadav, G. Nath, A. K. Srivastava and R. R. Yadav, *Mater. Chem. Phys.*, 2018, **218**, 10–17.
- 85 G. R. Salunke, S. Ghosh, R. J. Santosh Kumar, S. Khade, P. Vashisth, T. Kale, S. Chopade, V. Pruthi, G. Kundu, J. R. Bellare and B. A. Chopade, *Int. J. Nanomed.*, 2014, **9**, 2635–2653.
- 86 B. Syed, N. Karthik, P. Bhat, N. Bisht, A. Prasad, S. Satish and M. N. N. Prasad, *J. King Saud Univ., Sci.*, 2019, **31**, 798–803.
- 87 R. Dobrucka and J. Dlugaszewska, *Saudi Pharm. J.*, 2018, **26**, 643–650.
- 88 V. Jain, A. Khusnud, J. Tiwari, M. Mishra and P. K. Mishra, *Inorg. Nano-Met. Chem.*, 2021, **51**, 230–238.
- 89 G. M. de França Bettencourt, J. Degenhardt, L. A. Zevallos Torres, V. O. de Andrade Tanobe and C. R. Soccol, *Biocatal. Agric. Biotechnol.*, 2020, **30**, 101822.
- 90 R. Darabi, F. E. D. Alown, A. Aygun, Q. Gu, F. Gulbagca, E. E. Altuner, H. Seckin, I. Meydan, G. Kaymak, F. Sen and H. Karimi-Maleh, *Int. J. Hydrogen Energy*, 2023, **48**, 21270–21284.
- 91 F. Gulbagca, A. Aygun, E. E. Altuner, M. Bekmezci, T. Gur, F. Sen, H. Karimi-Maleh, N. Zare, F. Karimi and Y. Vasseghian, *Chem. Eng. Res. Des.*, 2022, **180**, 254–264.
- 92 J. Lin, F. Gulbagca, A. Aygun, R. N. Elhouda Tiri, C. Xia, Q. Van Le, T. Gur, F. Sen and Y. Vasseghian, *Food Chem. Toxicol.*, 2022, **163**, 112972.
- 93 A. Aygun, F. Gulbagca, E. E. Altuner, M. Bekmezci, T. Gur, H. Karimi-Maleh, F. Karimi, Y. Vasseghian and F. Sen, *Int. J. Hydrogen Energy*, 2023, **48**, 6666–6679.
- 94 K. Mallikarjuna, O. Nasif, S. Ali Alharbi, S. V. Chinni, L. V. Reddy, M. R. V. Reddy and S. Sreeramanan, *Biomolecules*, 2021, **11**, 190.
- 95 M. Ragothaman, B. T. Mekonnen and T. Palanisamy, *Mater. Chem. Phys.*, 2020, **253**, 123405.
- 96 D. M. Elsayed, S. M. Abdelbasir, H. M. Abdel-Ghafar, B. A. Salah and S. A. Sayed, *J. Environ. Chem. Eng.*, 2020, **8**, 103826.
- 97 V. K. Chaturvedi, N. Yadav, N. K. Rai, R. A. Bohara, S. N. Rai, L. Aleya and M. P. Singh, *Environ. Sci. Pollut. Res.*, 2021, **28**, 13761–13775.
- 98 Z. Oruç, M. Ergüt, D. Uzunoğlu and A. Özer, *J. Environ. Chem. Eng.*, 2019, **7**, 103231.



- 99 Health - United Nations Sustainable Development, <https://www.un.org/sustainabledevelopment/health/>, (accessed May 2023).
- 100 Y. M. Asi and C. Williams, *Int. J. Med. Inf.*, 2018, **114**, 114–120.
- 101 S. P. Singh and M. K. Singh, *Soil Pollution and Human Health BT - Plant Responses to Soil Pollution*, ed. P. Singh, S. K. Singh and S. M. Prasad, Springer, Singapore, 2020, pp. 205–220.
- 102 R. L. Hough, *Nat. Geosci.*, 2021, **14**, 183–184.
- 103 A. M. Badr, *Environ. Sci. Pollut. Res.*, 2020, **27**, 26036–26057.
- 104 W. Abdo, M. A. Elmadawy, E. Y. Abdelhice, M. A. Abdelkareem, A. Farag, M. Aboubakr, E. Ghazy and S. E. Fadl, *Sci. Rep.*, 2021, **11**, 2498.
- 105 M. Valcke, M. H. Bourgault, L. Rochette, L. Normandin, O. Samuel, D. Belleville, C. Blanchet and D. Phaneuf, *Environ. Int.*, 2017, **108**, 63–74.
- 106 X. Feng, L. Pan, J. Jing, J. Zhang, M. Zhuang, Y. Zhang, K. Wang and H. Zhang, *Sci. Total Environ.*, 2021, **773**, 145615.
- 107 Z. Khan, S. A. Al-Zahrani, Q. A. AlSulami, S. A. Al-Thabaiti and W. S. Al-Arjan, *J. Mol. Liq.*, 2019, **275**, 354–363.
- 108 H. R. Akbari Hasanjani and K. Zarei, *Microchem. J.*, 2021, **164**, 106005.
- 109 M. Badanthadka and H. M. Mehendale, *Encyclopedia of Toxicology*, 2014, pp. 896–899.
- 110 B. J. Curtis, J. R. West and J. Bridgeman, *Urban Water J.*, 2009, **6**, 407–415.
- 111 T. Sileshi, E. Tadesse, E. Makonnen and E. Aklillu, *Clin. Pharmacol.: Adv. Appl.*, 2021, **13**, 1–12.
- 112 K. Gopinath, C. Sundaravadivelan and A. Arumugam, *Int. J. Recent Sci. Res.*, 2013, **4**, 904–910.
- 113 O. Dumas, T. Despreaux, F. Perros, E. Lau, P. Andujar, M. Humbert, D. Montani and A. Descatha, *Respir. Med.*, 2018, **134**, 47–53.
- 114 B. T. Oba, X. Zheng, M. A. Aborisade, J. Liu, A. Yohannes, S. Kavwenje, P. Sun, Y. Yang and L. Zhao, *J. Environ. Manage.*, 2021, **285**, 112063.
- 115 K. Taddonio, N. Sherman and S. O. Andersen, in *WCX SAE World Congress Experience*, SAE International, 2019.
- 116 F. He, D. Zhao, J. Liu and C. B. Roberts, *Ind. Eng. Chem. Res.*, 2007, **46**, 29–34.
- 117 X. Wang, J. Xin, M. Yuan and F. Zhao, *Water Res.*, 2020, **183**, 116060.
- 118 Industrial Refrigeration Systems Market Size, Industrial Refrigeration Systems Market Size, Share & Trends Analysis Report By Component (Compressors, Condensers, Evaporators, Controls, Others), By Capacity, By Application, By Region, And Segment Forecasts, 2023–2030, *Grand View Research*, 2023.
- 119 J. Xue, Q. Xiao, M. Zhang, D. Li and X. Wang, *Int. J. Mol. Sci.*, 2023, **24**(13487).
- 120 C. Ohajinwa, P. van Bodegom, O. Osibanjo, Q. Xie, J. Chen, M. Vijver and W. Peijnenburg, *Int. J. Environ. Res. Public Health*, 2019, **16**, 906.
- 121 V. Linares, M. Bellés and J. L. Domingo, *Arch. Toxicol.*, 2015, **89**, 335–356.
- 122 X. Yang, Z. Sun, W. Wang, Q. Zhou, G. Shi, F. Wei and G. Jiang, *Sci. Total Environ.*, 2018, **643**, 559–568.
- 123 P. Wang, Y. N. Liang, Z. Zhong and X. Hu, *Sep. Purif. Technol.*, 2020, **233**, 115960.
- 124 G. Eichenbaum, M. Johnson, D. Kirkland, P. O'Neill, S. Stellar, J. Bielawne, R. DeWire, D. Areia, S. Bryant, S. Weiner, D. Desai-Krieger, P. Guzzie-Peck, D. C. Evans and A. Tonelli, *Regul. Toxicol. Pharmacol.*, 2009, **55**, 33–42.
- 125 R. Merugu, S. Garimella, R. Velamakanni, P. Vuppugalla, K. L. Chitturi and M. Jyothi, *Mater. Today: Proc.*, 2021, **44**, 153–156.
- 126 M. T. H. van Vliet, E. R. Jones, M. Flörke, W. H. P. Franssen, N. Hanasaki, Y. Wada and J. R. Yearsley, *Environ. Res. Lett.*, 2021, **16**, 024020.
- 127 UN-Water SDG 6 Data Portal, <https://www.sdg6data.org/en/node/1>, (accessed May 2023).
- 128 I. Kim, H. M. Yang, C. W. Park, I. H. Yoon, B. K. Seo, E. K. Kim and B. G. Ryu, *Sci. Rep.*, 2019, **9**, 10149.
- 129 M. Tumolo, V. Ancona, D. De Paola, D. Losacco, C. Campanale, C. Massarelli and V. F. Uricchio, *Int. J. Environ. Res. Public Health*, 2020, **17**, 5438.
- 130 Chromium in Drinking Water|US EPA, <https://www.epa.gov/sdwa/chromium-drinking-water>, (accessed May 2023).
- 131 G. Sharma, A. García-Peñas, A. Kumar, M. Naushad, G. T. Mola, S. M. Alshehri, J. Ahmed, N. Alhokbany and F. J. Stadler, *J. Mol. Liq.*, 2019, **285**, 362–374.
- 132 M. C. Danner, A. Robertson, V. Behrends and J. Reiss, *Sci. Total Environ.*, 2019, **664**, 793–804.
- 133 J. G. Navedo, V. Araya and C. Verdugo, *Sci. Total Environ.*, 2021, **777**, 146004.
- 134 Drinking Water and Pesticides|US EPA, <https://www.epa.gov/safepestcontrol/drinking-water-and-pesticides>, (accessed May 2023).
- 135 L. Petruzzi, M. R. Corbo, M. Sinigaglia and A. Bevilacqua, *The Microbiological Quality of Food: Foodborne Spoilers*, 2017, pp. 1–21.
- 136 M. Nasery, M. K. Hassanzadeh, Z. T. Najaran and S. A. Emami, *Essent. Oils Food Preserv., Flavor Saf.*, 2016, 659–665.
- 137 Sustainable consumption and production, <https://www.un.org/sustainabledevelopment/sustainable-consumption-production/>, (accessed May 2023).
- 138 S. Anand and M. K. Barua, *Comput. Electron. Agric.*, 2022, **198**, 106936.
- 139 S. Santacruz and J. Cedeño, *Rev. Fac. Nac. Agron. Medellin*, 2021, **74**, 9615–9619.
- 140 State of Food Agriculture 2019, Moving forward on food loss and waste reduction, Policy Support and Governance, Food and Agriculture Organization of the United Nations, <https://www.fao.org/policy-support/tools-and-publications/resources-details/en/c/1242090/>, (accessed May 2023).
- 141 Food and Agriculture Organization of the United Nations (FAO), Preventing *E. coli* in *Food*, 2011.
- 142 S. Z. Mirzaei, S. Ahmadi Somaghian, H. E. Lashgarian, M. Karkhane, K. Cheraghpour and A. Marzban, *Ceram. Int.*, 2021, **47**, 5580–5586.



- 143 S. Salari and S. M. Jafari, *Trends Food Sci. Technol.*, 2020, **97**, 100–113.
- 144 B. Amrutha, K. Sundar and P. H. Shetty, *J. Food Sci. Technol.*, 2017, **54**, 1091–1097.
- 145 P. R. Neves, J. A. McCulloch, E. M. Mamizuka and N. Lincopan, *Encyclopedia of Food Microbiology*, 2nd edn, 2014, pp. 253–260.
- 146 B. Ellison, *Am. J. Agric. Econ.*, 2020, **102**, 1047–1049.
- 147 F. Mneimneh, H. Ghazzawi, M. Abu Hejjeh, M. Manganelli and S. Ramakrishna, *Energies*, 2023, **16**, 1368.
- 148 M. V. S. Sandhya, K. Rajkumar and S. Burgula, *Green Chem. Lett. Rev.*, 2019, **12**, 420–434.
- 149 H. Adam and A. Youssef, *SSRN Electron. J.*, 2019.
- 150 I. M. Radwan, A. Gitipour, P. M. Potter, D. D. Dionysiou and S. R. Al-Abed, *J. Nanopart. Res.*, 2019, **21**, 155.
- 151 The Project on Emerging Nanotechnologies, Consumer Products Inventory, <https://www.nanotechproject.tech/cpi/>, (accessed November 2023).
- 152 The Ecological Council, DTU and Taenk Forbugerradet, The Nanodatabase, <https://nanodb.dk/>, (accessed November 2023).
- 153 A. Shan, M. Cheng, H. Fan, Z. Chen, R. Wang and C. Chen, *Prog. Nat. Sci.: Mater. Int.*, 2014, **24**, 175–178.
- 154 V. Nagpal, A. D. Bokare, R. C. Chikate, C. V. Rode and K. M. Paknikar, *J. Hazard. Mater.*, 2010, **175**, 680–687.
- 155 N. Zhou, Y. Liu, J. Shen, X. Chu, Z. Pan, Q. Song, Y. Wang, W. Feng, S. Shi and W. Xu, *CN Pat.*, CN113016823B, 2022.
- 156 L. Li, D. H. Anjum, L. Zhou, P. Laveille and J. Basset, *US Pat.*, US10537881B2, 2021.
- 157 D. Jiang, G. Zeng, D. Huang, C. Lai, P. Xiao, C. Zheng, M. Cheng, Y. Liu, J. Wan, W. Xue and H. Wang, *CN Pat.*, CN109200988B, 2020.
- 158 U. Park, S. Young, S. Yong, T. Yong and H. Y. Yong, *JP Pat.*, JP6408636B2, 2018.
- 159 S. Kabtani, D. Sdouga, I. Bettaib Rebey, M. Save, N. Trifi-Farah, M. L. Fauconnier and S. Marghali, *Sci. Rep.*, 2020, **10**, 8293.
- 160 S. Davarpanah, A. Tehranifar, M. Zarei, M. Aran, G. Davarynejad and J. Abadía, *Agronomy*, 2020, **10**, 832.
- 161 H. T. Phan and A. J. Haes, *J. Phys. Chem. C*, 2019, **123**, 16495–16507.
- 162 A. Scala, G. Neri, N. Micale, M. Cordaro and A. Piperno, *Molecules*, 2022, **27**, 1134.
- 163 Z. Jiang, Q. Zhang, C. Zong, B. J. Liu, B. Ren, Z. Xie and L. Zheng, *J. Mater. Chem.*, 2012, **22**, 18192–18197.
- 164 Z. Zhuang, F. Wang, R. Naidu and Z. Chen, *J. Power Sources*, 2015, **291**, 132–137.
- 165 L. Berta, N. A. Coman, A. Rusu and C. Tanase, *Materials*, 2021, **14**, 7677.
- 166 S. Krishnan Sundarrajan and L. Pottail, *Appl. Nanosci.*, 2021, **11**, 971–981.
- 167 C. Song, S. Sun, J. Wang, Y. Gao, G. Yu, Y. Li, Z. Liu, W. Zhang and L. Zhou, *Front. Microbiol.*, 2023, **13**, 1–17.
- 168 S. Aliyari Rad, K. Nobaharan, N. Pashapoor, J. Pandey, Z. Dehghanian, V. Senapathi, T. Minkina, W. Ren, V. D. Rajput and B. Asgari Lajayer, *Sustain*, 2023, **15**, 1–19.
- 169 L. Yang, X. Jin, Q. Lin, G. Owens and Z. Chen, *Sep. Purif. Technol.*, 2023, **311**, 123249.
- 170 J. Chen, Y. Guo, X. Zhang, J. Liu, P. Gong, Z. Su, L. Fan and G. Li, *J. Agric. Food Chem.*, 2023, **71**, 3564–3582.
- 171 D. Lomelí-Marroquín, D. Medina-Cruz, A. Nieto-Argüello, A. Vernet-Crua, J. Chen, A. Torres-Castro, T. J. Webster and J. L. Cholula-Díaz, *Int. J. Nanomed.*, 2019, **14**, 2171–2190.
- 172 R. Gupta and H. Xie, *J. Environ. Pathol., Toxicol. Oncol.*, 2018, **37**, 209–230.
- 173 Nanotechnology Research Center (NTRC), <https://www.cdc.gov/niosh/programs/nano/default.html>, (accessed November 2023).
- 174 K. Ulucan-Altuntas, A. El Hadki, L. Bilgili, A. Y. Çetinkaya, S. L. Kuzu and E. Debik, *Water, Air, Soil Pollut.*, 2022, **233**, 1–12.
- 175 C. Visentin, A. W. da S. Trentin, A. B. Braun and A. Thomé, *Environ. Pollut.*, 2021, **268**, 115915.
- 176 B. Salieri, D. A. Turner, B. Nowack and R. Hischer, *NanoImpact*, 2018, **10**, 108–120.

